March, 2011

Patatin-Related Phospholipase pPLAIIIβ-Induced Changes in Lipid Metabolism Alter Cellulose Content and Cell Elongation in Arabidopsis

Xuemin Wang, *University of Missouri-St. Louis*
Maoyin Li, *University of Missouri–St. Louis*
Sung Chul Bahn
Liang Guo, *University of Missouri–St. Louis*
William Musgrave, et al.

The Plant Cell, Vol. 23: 1107–1123, March 2011, www.plantcell.org © 2011 American Society of Plant Biologists

Patatin-Related Phospholipase pPLAIIIβ-Induced Changes in Lipid Metabolism Alter Cellulose Content and Cell Elongation in *Arabidopsis* [C][W]

Maoyin Li,[a,b] Sung Chul Bahn,[a,b] Liang Guo,[a,b] William Musgrave,[b] Howard Berg,[b] Ruth Welti,[c] and Xuemin Wang[a,b,1]

[a] Department of Biology, University of Missouri, St. Louis, Missouri 63121
[b] Donald Danforth Plant Science Center, St. Louis, Missouri 63132
[c] Kansas Lipidomics Research Center, Division of Biology, Kansas State University, Manhattan, Kansas 66506

The release of fatty acids from membrane lipids has been implicated in various plant processes, and the patatin-related phospholipases (pPLAs) constitute a major enzyme family that catalyzes fatty acid release. The *Arabidopsis thaliana pPLA* family has 10 members that are classified into three groups. Group 3 *pPLAIII* has four members but lacks the canonical lipase/esterase consensus catalytic sequences, and their enzymatic activity and cellular functions have not been delineated. Here, we show that pPLAIIIβ hydrolyzes phospholipids and galactolipids and additionally has acyl-CoA thioesterase activity. Alterations of *pPLAIIIβ* result in changes in lipid levels and composition. *pPLAIIIβ*-KO plants have longer leaves, petioles, hypocotyls, primary roots, and root hairs than wild-type plants, whereas *pPLAIIIβ*-OE plants exhibit the opposite phenotype. In addition, *pPLAIIIβ*-OE plants have significantly lower cellulose content and mechanical strength than wild-type plants. Root growth of *pPLAIIIβ*-KO plants is less sensitive to treatment with free fatty acids, the enzymatic products of pPLAIIIβ, than wild-type plants; root growth of *pPLAIIIβ*-OE plants is more sensitive. These data suggest that alteration of *pPLAIIIβ* expression and the resulting lipid changes alter cellulose content and cell elongation in *Arabidopsis*.

INTRODUCTION

Phospholipases participate in many aspects of cellular function by generating lipid messengers, modifying membrane composition, and modulating the physical properties of membranes (Wang, 2001; Meijer and Munnik, 2003; Ryu, 2004; Li et al., 2009; Matos and Pham-Thi, 2009; Scherer et al., 2010). Phospholipases are classified into A-types (PLA), C-types (PLC), and D-types (PLD) based on the site at which hydrolysis of the phospholipid molecule is catalyzed (Wang 2001). PLA_2 comprises mainly cytosolic Ca^{2+}-dependent PLA_2 ($cPLA_2$), Ca^{2+}-indepenedent PLA_2 ($iPLA_2$), and secreted PLA_2 in animal cells (Six and Dennis, 2000). $iPLA_2$ and $cPLA_2$ are patatin-related enzymes. In *Arabidopsis thaliana*, 10 genes have been identified as encoding patatin-related phospholipase A enzymes, designated as *pPLA* (Scherer et al., 2010).

The 10 members of the *pPLA* family are classified into three groups: *pPLAI*, *pPLAII* (α, β, γ, δ, and ε), and *pPLAIII* (α, β, γ, and δ), based on their deduced amino acid sequence and gene structure (Scherer et al., 2010). *pPLAI* is the only gene/protein in group 1 with three conserved domains, a C-terminal leucine-rich repeat domain, an N-terminal weak ankyrin-like homology domain, and an enzymatic domain, which is homologous to enzymatic domains of animal $iPLA_2\alpha$ and other pPLAs. The recognizable homology to animal *$iPLA_2$*s may indicate that *pPLAI* is the *pPLA* most similar to the common ancestral gene. *pPLAII*s and *pPLAIII*s differ from each other in several ways. *pPLAII*s are more closely related to potato (*Solanum tuberosum*) tuber patatin than *pPLAIII*s. *pPLAII* genes, like that of *pPLAI*, contain five to six introns, whereas those of *pPLAIII* have only one intron. *pPLAII* genes are similar to the region of animal *$iPLA_2$* genes that encode the catalytic domains. pPLAI and pPLAII have the canonical lipase/esterase S-D dyad consensus catalytic sequences, but pPLAIIIs do not. pPLAI and pPLAIIs have been shown to hydrolyze phospholipids and galactolipids, but not triacylglycerol, in vitro (La Camera et al., 2005; Yang et al., 2007; Rietz et al., 2010). However, no enzymatic activity of pPLAIIIs has been reported thus far, raising the question as to whether *pPLAIII*s encode active acyl-hydrolyzing enzymes.

pPLAs have been implicated in several physiological functions, particularly in the plant's response to pathogens, auxin, and phosphate deficiency. *pPLAI* may mediate the basal levels of jasmonate (JA) production and contribute to the resistance to *Botrytis cinerea* (Yang et al., 2007). *pPLAIIα* is involved in plant-bacterial pathogen interactions (Rietz et al., 2004; La Camera et al., 2005). *pPLAIIβ* facilitates the plant's response to phosphate deficiency during root elongation, whereas *pPLAIIγ* is important in the auxin response (Rietz et al., 2010). *pPLAIIδ* is also induced by auxin (Rietz et al., 2010). In contrast with groups 1 and 2 *pPLA*s, little is known about the involvement of *pPLAIII*s in plant processes. During a screen for lodging resistant plants,

[1] Address correspondence to wangxue@umsl.edu.
The author responsible for distribution of materials integral to the findings presented in this article in accordance with the policy described in the Instructions for Authors (www.plantcell.org) is: Xuemin Wang (wangxue@umsl.edu).
[C]Some figures in this article are displayed in color online but in black and white in the print edition.
[W]Online version contains Web-only data.
www.plantcell.org/cgi/doi/10.1105/tpc.110.081240

an activation-tagged mutant of *pPLAIIIδ*, designated *STURDY*, was isolated; it displayed a stiff inflorescence stalk, thick leaves, and large seeds (Huang et al., 2001).

Here, we characterize the enzymatic properties and cellular functions of *pPLAIIIβ*. The data show that pPLAIIIβ possesses acyl-hydrolyzing activity on phospholipids and galactolipids and also acyl-CoA thioesterase activity. Genetic manipulation of *pPLAIIIβ* alters *Arabidopsis* growth, lipid levels, cellulose content, and mechanical strength. Further analysis of *pPLAIIIβ*-altered plants indicates that pPLAIIIβ and the free fatty acids (FFAs) it produces are involved in the regulation of longitudinal cell growth. The results suggest that changes in *pPLAIIIβ* expression and the resulting lipid changes play a role in lipid metabolism, cell morphogenesis, and carbon partitioning between lipids and cellulose.

RESULTS

pPLAIIIs Lack the Canonical S-D Dyad Esterase Motif and Are Expressed Differentially

pPLAI and pPLAII have the canonical sequences in their catalytic centers, including the esterase box *GxSxG*, the phosphate or anion binding element *DGGGxxG*, and the catalytic dyad-containing motif *DGG* or *DGA* (Figure 1A). However, in pPLAIII proteins, the corresponding sequence of the esterase box is *GxGxG*, and the missing Ser in the *GxSxG* box is recognized as a critical amino acid in the S-D catalytic dyad (Figure 1A). The Asp (D) residue in the conserved *DGG* motif was replaced by Gly (G) in pPLAIIIβ; the Asp residue is important for the formation of the catalytic dyad in PLA (Figure 1A).

The transcript levels of *pPLAIIIs* were determined by quantitative real-time PCR in *Arabidopsis* tissues using reference genes UBQ10 and β-tubulin and by analyzing microarray data from Genevestigator (Figures 1B to 1D). *pPLAIIIβ* expression was relatively high in roots and old leaves and low in siliques, while *pPLAIIIα* expression was particularly high in siliques. *pPLAIIIβ* was also expressed in young leaves, inflorescences, and flowers, whereas *pPLAIIIγ* and *pPLAIIIδ* were hardly expressed in leaves. *pPLAIIIγ* and *pPLAIIIδ* were primarily expressed in roots. The expression pattern as determined by real-time PCR and Genevestigator were comparable (Figures 1B to 1D). Overall, the four *pPLAIII* genes varied in tissue expression pattern.

pPLAIIIβ was expressed at various developmental stages, including germinated seeds, seedlings, young rosettes, developed rosettes, bolting, young flowers, developed flowers, developing siliques, and mature siliques, and the level of expression is comparable in most stages, except that a lower level occurred in young and developed rosettes (see Supplemental Figure 1A online). The expression of *pPLAIIIβ* was increased approximately twofold in response to auxin (indole-3-acetic acid), but the level of *pPLAIIIβ* expression was not changed in response to abscisic acid, methyl jasmonate, JA, 12-oxo-phytodienoic acid (OPDA), phosphorous deficiency, wounding, and iron deficiency (see Supplemental Figures 1B and 1C online).

pPLAIIIβ Encodes an Active Acyl-Hydrolyzing Enzyme

To determine whether *pPLAIIIs* encode functional acyl-hydrolyzing enzymes, we cloned *pPLAIIIβ* cDNA, tagged it at the C terminus with polyhistidine (6xHis), and expressed it in *Escherichia coli* (Figure 2A). Purified pPLAIIIβ was assayed for acyl-hydrolyzing activity using the conditions previously defined for pPLAI (Yang et al., 2007). When 16:0-18:2 phosphatidylcholine (PC) was used as a substrate, free 16:0 and 18:2 fatty acids were released (Figure 2B). The generation of FFAs increased as a function of the incubation time with the purified enzyme but not with vector control protein. Concomitant production of lysophosphatidylcholine (LPC), 16:0-LPC, and 18:2-LPC was also observed (Figure 2C). The release of 18:2 from the sn-2 position is approximately sixfold greater than that of 16:0 from the sn-1 position. Consistent with the acyl release, the production of 1-acyl 16:0-LPC was also much greater than 2-acyl 18:2-LPC. The results suggest that pPLAIIIβ prefers the sn-2 to the sn-1 position in PC hydrolysis.

Next, we examined whether pPLAIIIβ has activity toward other classes of phospholipids, including phosphatidylethanolamine (PE), phosphatidylserine (PS), phosphatidic acid (PA), and phosphatidylglycerol (PG). pPLAIIIβ hydrolyzed all the phospholipids tested, and the highest activity was detected with PG as a substrate (Figure 2D). When galactolipids, monoglactosyldiacylglycerol (MGDG), and digalactosyldiacylglycerol (DGDG) were used, the activity of pPLAIIIβ toward DGDG was approximately fourfold greater than that toward MGDG (Figure 2D). When neutral lipids, diacylglycerol and triacylglycerol, were tested, no fatty acid release was detected. However, free 18:3 was released from 18:3-CoA by purified pPLAIIIβ but not by vector control protein (Figure 2E). The production of free 18:3 fatty acid increased as a function of incubation time (Figure 2F). This result indicates that pPLAIIIβ possesses acyl-CoA thioesterase activity.

To further verify the activity of pPLAIIIβ, the protein was tagged at the C terminus with green fluorescent protein and polyhistidine (GFP-His) and expressed in *Arabidopsis* (Figure 3A). GFP-His–tagged pPLAIIIβ was isolated from plants and its activity was assayed. When 16:0-18:2 PC was used as a substrate, the FFAs (16:0 and 18:2) were generated after incubation with purified pPLAIIIβ but not with protein from vector control plants (Figure 3B). More 18:2 was released from the sn-2 position than 16:0 from the sn-1 position, consistent with the activity of pPLAIIIβ produced from *E. coli*. To test acyl-CoA thioesterase activity, equal amounts of 18:2-CoA and 18:3-CoA were mixed and used as substrate. Both FFAs, 18:2 and 18:3, were produced when the acyl-CoAs were incubated with tagged pPLAIIIβ but not with the vector control protein; hydrolysis of the two acyl-CoAs was similar (Figure 3C).

Overexpression of *pPLAIIIβ* Increased, Whereas Knockout Decreased, Lipid Content

To determine pPLAIIIβ function in lipid metabolism in vivo, we produced *Arabidopsis* transgenic lines that overexpress *pPLAIIIβ* (*pPLAIIIβ*-OE) under the control of the 35S promoter (Figure 3A). We also isolated a T-DNA insertion knockout mutant

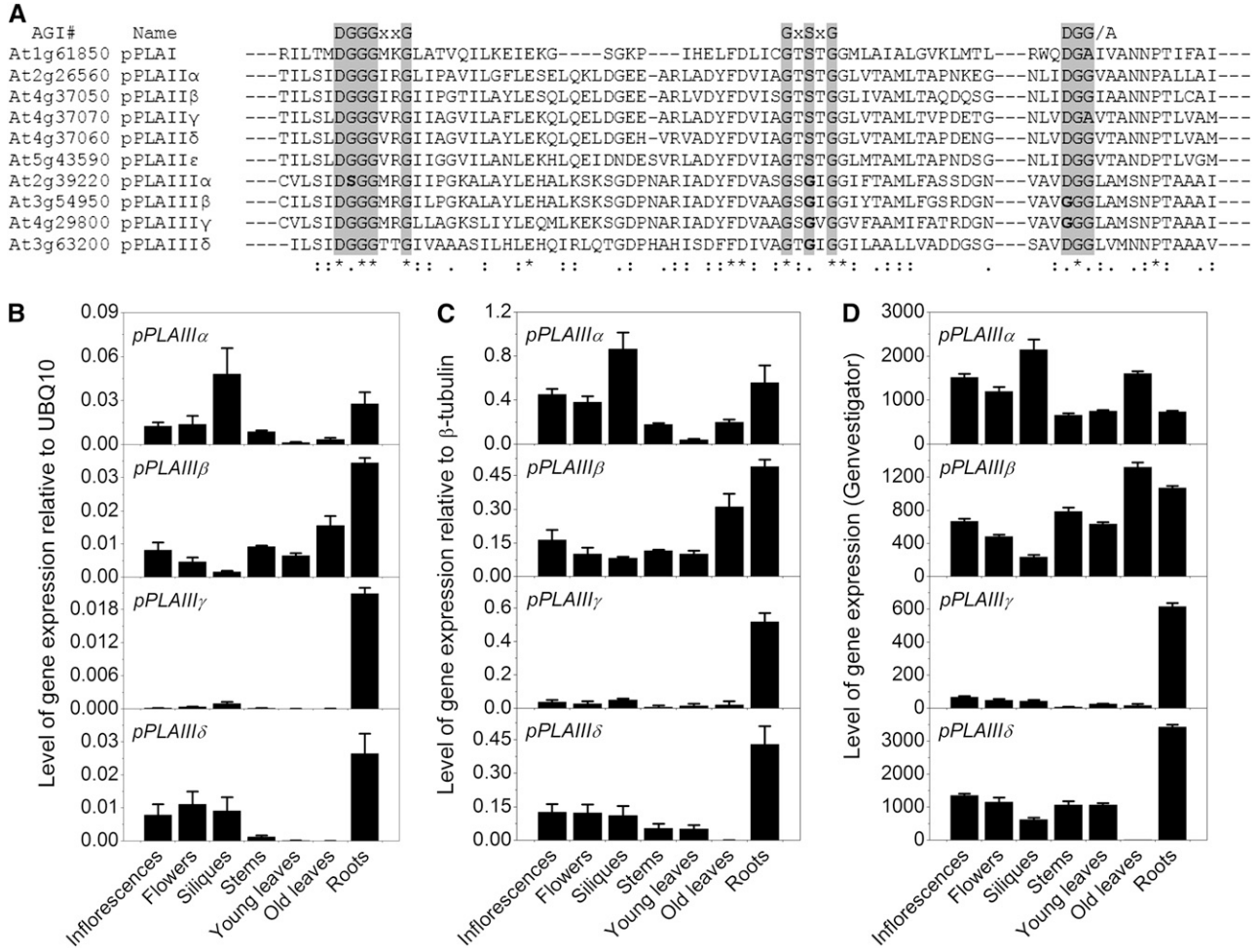

Figure 1. Alignment of 10 pPLAs and Gene Expression of *pPLAIII*s.

(A) Alignment of deduced amino acid sequences of plant patatin-like acyl-hydrolase families (pPLAs) in *Arabidopsis*. Ten *Arabidopsis* genes encode pPLAs, and these are classified into three groups (Scherer et al., 2010). Group 1 has one gene, *pPLAI*; group 2 has five genes, *pPLAIIα*, *β*, *γ*, *δ*, and *ε*; and group 3 has four genes, *pPLAIIIα*, *β*, *γ*, and *δ*. The catalytic center is marked; this includes the esterase box *GxSxG* (in pPLAIIIα, β, γ, and δ, it is *GxGxG*), the phosphate or anion binding element *DGGGxxG*, and the catalytic dyad-containing motif *DGG* or *DGA* (in pPLAIIIβ and γ, it is *GGG*). The protein sequences were aligned using the website http://www.ebi.ac.uk/Tools/clustalw2/index.html, and the conserved domains were identified using the website http://www.ncbi.nlm.nih.gov/Structure/cdd.shtml. The gray highlighting indicates the region of conserved motif. The bold highlighting indicates the different amino acids in the conserved motif.

(B) Expression of group 3 *pPLA*s, *pPLAIIIα*, *pPLAIIIβ*, *pPLAIIIγ*, and *pPLAIIIδ*, in seven types of *Arabidopsis* tissues, as quantified by real-time PCR normalized to *ubiquitin10* (*UBQ10*). Values are means ± SD (*n* = 3 technical replicates).

(C) Expression of group 3 *pPLA*s, *pPLAIIIα*, *pPLAIIIβ*, *pPLAIIIγ*, and *pPLAIIIδ*, in seven types of *Arabidopsis* tissues, as quantified by real-time PCR normalized to *β-tubulin*. Values are means ± SD (*n* = 3 technical replicates).

(D) Expression of group 3 *pPLA*s, *pPLAIIIα*, *pPLAIIIβ*, *pPLAIIIγ*, and *pPLAIIIδ*, in seven types of *Arabidopsis* tissues based on data from Genevestigator (http://www.genevestigator.com). Values are means ± SD (*n* = 5 independent experiments).

(*pPLAIIIβ*-KO) and genetically complemented the knockout (KO) mutant with the native *pPLAIIIβ* (*pPLAIIIβ*-COM) (Figure 4A). The *pPLAIIIβ* transcript was undetectable in *pPLAIIIβ*-KO, while complementation (*pPLAIIIβ*-COM) restored expression of *pPLAIIIβ* in the *pPLAIIIβ*-KO background (Figure 4B). The expression level in *pPLAIIIβ*-OE mutants was 100 times more than in the wild type (Figure 4B). Production of pPLAIIIβ in OE plants was detected by immunoblotting with antibody against the GFP tag (Figure 3A). Thus, KO eliminated expression of *pPLAIIIβ*, OE greatly increased it, and COM had the same level of *pPLAIIIβ* expression as the wild type.

Lipids were extracted from the 2-week-old rosettes of the wild type, KO, OE, and COM, and lipid profiling was performed by mass spectrometry. FFAs and lysophospholipids are potential products of the enzyme. Indeed, the total FFA level was 20% lower in KO and 15% higher in OE than in the wild type (Figure 4C). In *Arabidopsis* leaves, the most abundant FFAs were polyunsaturated species (Figure 4D). 18:3 linolenic acid constituted

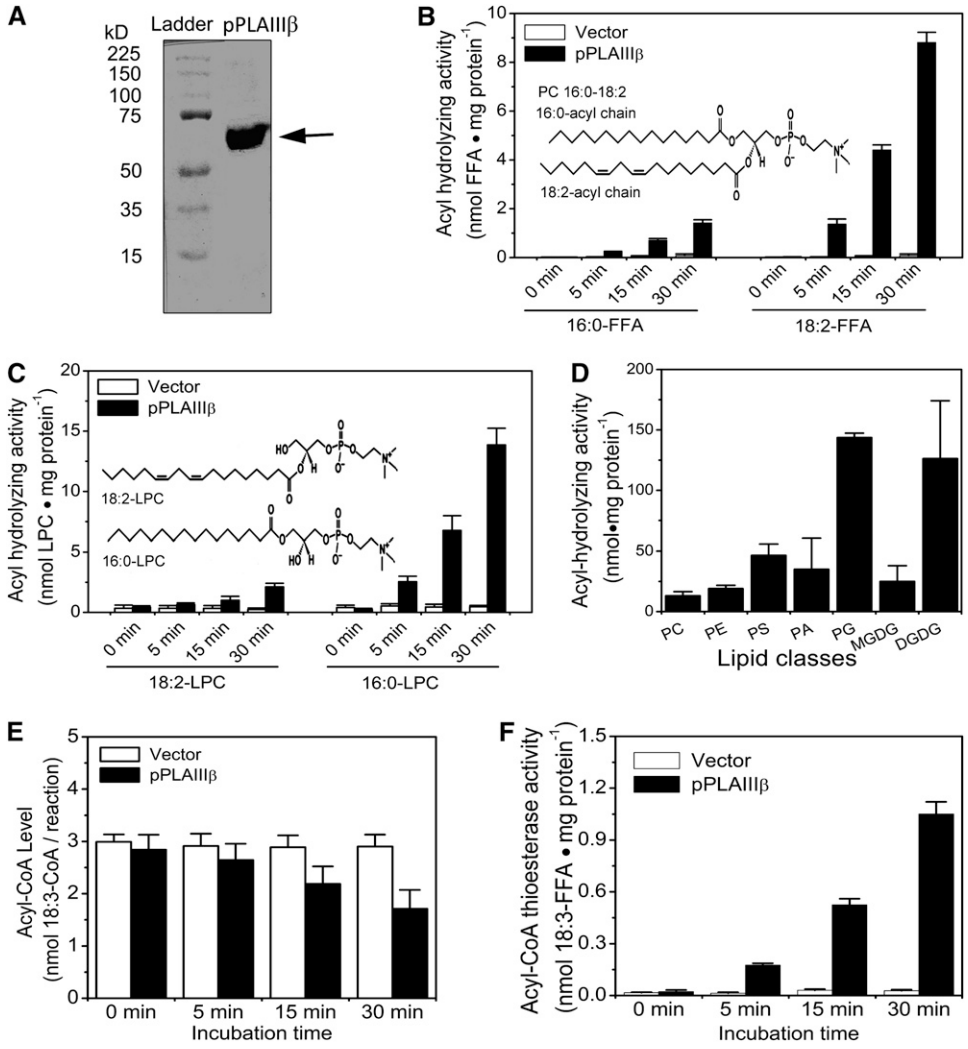

Figure 2. Acyl Hydrolyzing Activity of Bacterially Expressed pPLAIIIβ.

(A) Coomassie blue staining of an 8% SDS-PAGE gel loaded with affinity-purified His-tagged pPLAIIIβ (arrow) from *E. coli*.

(B) FFA released by pPLAIIIβ when 16:0-18:2 PC [1-hexadecanoyl-2-(9Z,12Z-octadecadienoyl)-*sn*-glycero-3-phosphocholine] vesicles were used as a substrate. Inset: structure of 16:0-18:2 PC. Values are means ± SD (n = 3 separate samples).

(C) LPC released by pPLAIIIβ when 16:0-18:2 PC vesicles were used as a substrate. Inset: structures of 16:0-LPC and 18:2-LPC. Values are means ± SD (n = 3 separate samples).

(D) Acyl hydrolysis activity of pPLAIIIβ toward various classes of phospholipids and galactolipids. Vesicles made from individual lipid species were incubated with pPLAIIIβ at 30°C for 30 min. After the reaction, lipids were extracted and quantified by ESI-MS/MS (Welti et al., 2002). Values are means ± SD (n = 3 separate samples).

(E) Acyl-CoA substrate decreased after incubation with pPLAIIIβ. 18:3-CoA was hosted in 16:0-18:2 PC vesicles and incubated with pPLAIIIβ for the indicated amount of time. After the reaction, acyl-CoA was quantified by ESI-MS/MS in neutral loss mode as described in Methods. Values are means ± SD (n = 3 separate samples).

(F) FFA released by pPLAIIIβ when 18:3-CoA (6*Z*,9*Z*,12*Z*-octadecatrienoyl CoA), hosted in 16:0-18:2 PC vesicles, was used as a substrate. Vector refers to a control in which proteins from *E. coli* transformed with an empty vector were isolated using the same immunoaffinity procedure used to isolate pPLAIIIβ-His. Values are means ± SD (n = 3 separate samples).

50% and 16:3 and 18:2 linoleic acid made up of 15 and 5%, respectively, of the total FFAs. All FFA species exhibited a tendency to decrease in KO and increase in OE compared with the wild type (Figure 4D). The level of total lysophospholipids was 15% higher in OE than in the wild type (Figure 4E). The level of lysophospholipid species of KO was comparable to that of the wild type but tended to be higher in OE (Figures 4E and 4F). Fatty acid compositions were measured in the mature seeds of wild-type, KO, OE, and COM plants. The level of 20:1 was significantly lower in KO and higher in OE seeds, whereas the levels of 18:2

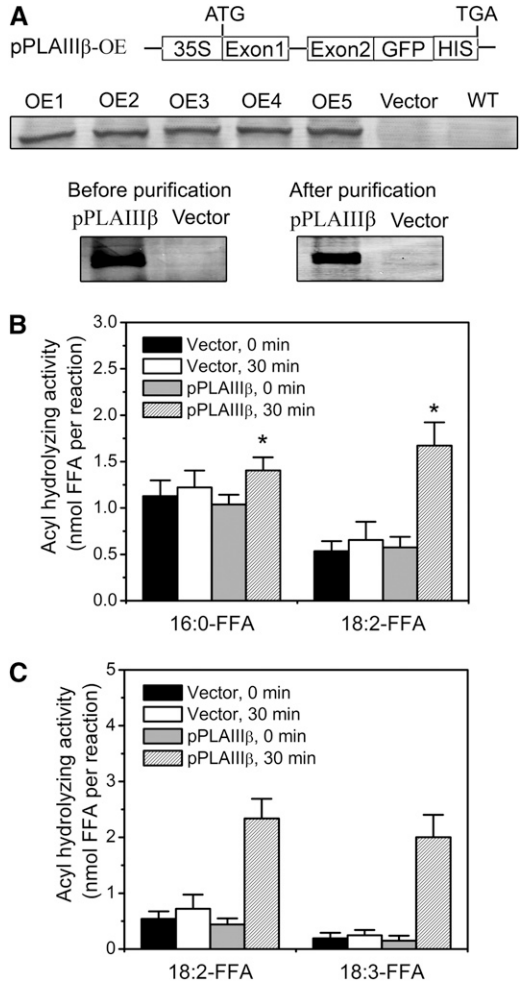

Figure 3. pPLAIIIβ Expression in *Arabidopsis*.

(A) Production of His-tagged pPLAIIIβ in *Arabidopsis*. The pPLAIIIβ genomic DNA sequence was cloned into a vector with the constitutive expression promoter 35S and in frame with the GFP-His tag in the C terminus. Leaf proteins extracted from pPLAIIIβ-GFP-His transgenic plants were separated by 8% SDS-PAGE and transferred to a polyvinylidene difluoride membrane. Lanes 1 through 5 represent different transgenic lines carrying the pPLAIIIβ-GFP-His overexpression construct. The pPLAIIIβ-GFP-His–tagged protein was purified from leaves using NTA agarose beads (Qiagen) and then visualized with alkaline phosphatase conjugated to a secondary anti-mouse antibody after blotting with GFP antibody.

(B) Acyl hydrolyzing activity of pPLAIIIβ. pPLAIIIβ-GFP-His, purified from plant leaves using NTA agarose beads, was incubated with vesicles of 16:0-18:2 PC for 30 min at 30°C with gentle shaking. After the reaction, the lipids were extracted, and FFAs were quantified by ESI-MS scans. Values are means ± SD (n = 3) of three independent experiments. Asterisk indicates significant difference at $P < 0.05$ compared between 0 and 30 min of pPLAIIIβ incubation based on Student's t test.

(C) Fatty acyl-CoA thioesterase activity of pPLAIIIβ. Purified pPLAIIIβ-GFP-His protein from plant leaves was incubated with equal amounts of linoleoyl CoA and 6*Z*,9*Z*,12*Z*-octadecatrienoyl CoA (18:2-CoA and 18:3-CoA) hosted in 16:0-18:1 PC vesicles for 30 min at 30°C with gentle shaking. Released FFAs were extracted and quantified by ESI-MS scans. Each data point represents the average ± SD from three separate determinations.

and 18:3 tended to be higher in KO and lower in OE but not significantly (see Supplemental Figure 2A online). C29 alkane and C29 ketone are two major components of cuticular wax, representing 80% of the total cuticular wax load in stems (Li-Beisson, 2010). OE plants tended to have a higher level of C29 alkane and C29 ketone in stem cuticles than the wild type and KO (see Supplemental Figure 2B online).

The level of total lipids, including phospholipids and galactolipids, was significantly lower in KO but 15% higher in OE than in the wild type (Figures 5A to 5C). There was a general trend toward the content of various classes of lipids being lower in KO but higher in OE compared with the wild type. Genetic complementation of the KO mutant with the *pPLAIIIβ* gene (COM) restored the lipid levels to wild-type levels, confirming that the lipid alterations resulted from the loss of function of *pPLAIIIβ*. For most molecular species, except PS species and lysophospholipid species, the levels were lower in KO and higher in OE than the wild type. The levels of 34:3 PS, 42:3 PS, and 42:4 PS were lower in OE than in the wild type (Figure 5C).

pPLAIIIβ Is Associated with the Plasma Membrane

To determine the localization of pPLAIIIβ, GFP-tagged pPLAIIIβ was imaged in leaf epidermal cells by confocal microscopy. Green fluorescence was detected in OE epidermal cells but not in the wild type (Figure 6A, panels b and f). The green fluorescent signal was coincident with the cell border but not with the red fluorescent signal from chloroplasts (Figure 6A, panels e to h). To test whether pPLAIIIβ was associated with the cell wall, plasmolysis in root cells was induced with salinity. After plasmolysis, the GFP signal moved with the protoplast, indicating that it was not wall associated (Figure 6B, right panel).

To verify the intracellular localization, transgenic *Arabidopsis* leaves were fractionated and GFP-His–tagged pPLAIIIβ was detected by immunoblotting of subcellular fractions. pPLAIIIβ was present in the microsomal but not in the soluble fractions (Figure 6C). When the microsomal membranes were separated into the plasma membrane and intracellular membrane fractions, most pPLAIIIβ was associated with the plasma membrane (Figure 6C). Most PC acyl hydrolase activity due to pPLAIIIβ overexpression was also associated with the plasma membrane (Figure 6D). Together, these data indicate that pPLAIIIβ is associated with the plasma membrane.

Alterations of *pPLAIIIβ* Alter Plant Size and Morphology

Genetic alterations in the level of *pPLAIIIβ*, particularly overexpression of *pPLAIIIβ*, resulted in morphological changes of *Arabidopsis* plants. The plant size of all OE lines was smaller, whereas that of KO was slightly larger than that of the wild type after 2 weeks of growth in soil (Figure 7A). The smaller stature of *pPLAIIIβ*-OE persisted throughout its life span (see Supplemental Figure 3 online). Compared with the wild type, the OE rosettes were more compact and the leaves were smaller (Figures 7A and 7B). The stalks of the OE plants were shorter (see Supplemental Figures 3C and 3D online) but wider than those of the wild type (Figure 7C), and siliques were also shorter (Figure 7D) but wider than the wild type (see Supplemental Figure 3E online). The

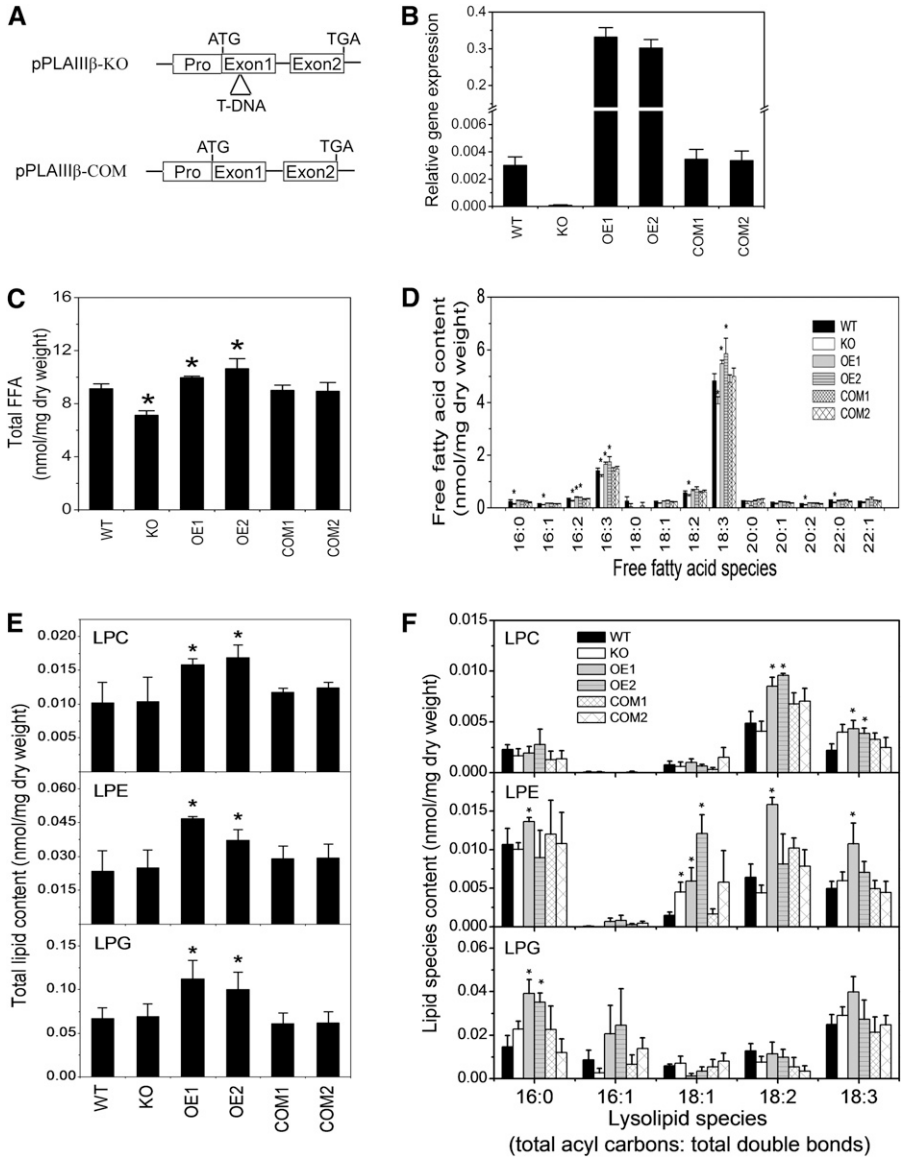

Figure 4. The Effect of *pPLAIIIβ* Alterations on Lipid Content of FFA and Lysophospholipids in *Arabidopsis*.

Lipids were extracted from 2-week-old soil-grown plant rosettes and analyzed by ESI-MS/MS as described by Xiao et al. (2010). Asterisk indicates a significant difference between mutant plants and wild-type plants with $P < 0.05$ in the Student's *t* test.

(A) T-DNA insertion site in the *pPLAIIIβ* gene and the complementation construct introduced into the T-DNA insertion mutant. Boxes denote exons and lines introns.

(B) Determination of *pPLAIIIβ* transcript in the wild type, knockout line (*pPLAIIIβ*-KO), overexpression lines (*pPLAIIIβ*-OE), and complementation line (*pPLAIIIβ*-COM). The expression levels were normalized in comparison to *UBQ10*. Values are means ± SD ($n = 3$ technical replicates).

(C) Total FFAs in wild-type, KO, OE, and COM lines, showing the reduced FFA content of KO and the increased FFA content of OE plants compared with the wild type. Values are means ± SD ($n = 5$ separate samples).

(D) FFA molecular species in wild-type, KO, OE, and COM mutants. Values are means ± SD ($n = 5$ separate samples).

(E) Total lysophospholipid content in wild-type, KO, OE, and COM lines. Lysophospholipids include LPC, LPE, and LPG. Values are means ± SD ($n = 5$ separate samples).

(F) Lysophospholipid molecular species in wild-type, KO, OE, and COM mutants. Lysophospholipids include LPC, LPE, and LPG. Values are means ± SD ($n = 5$ separate samples).

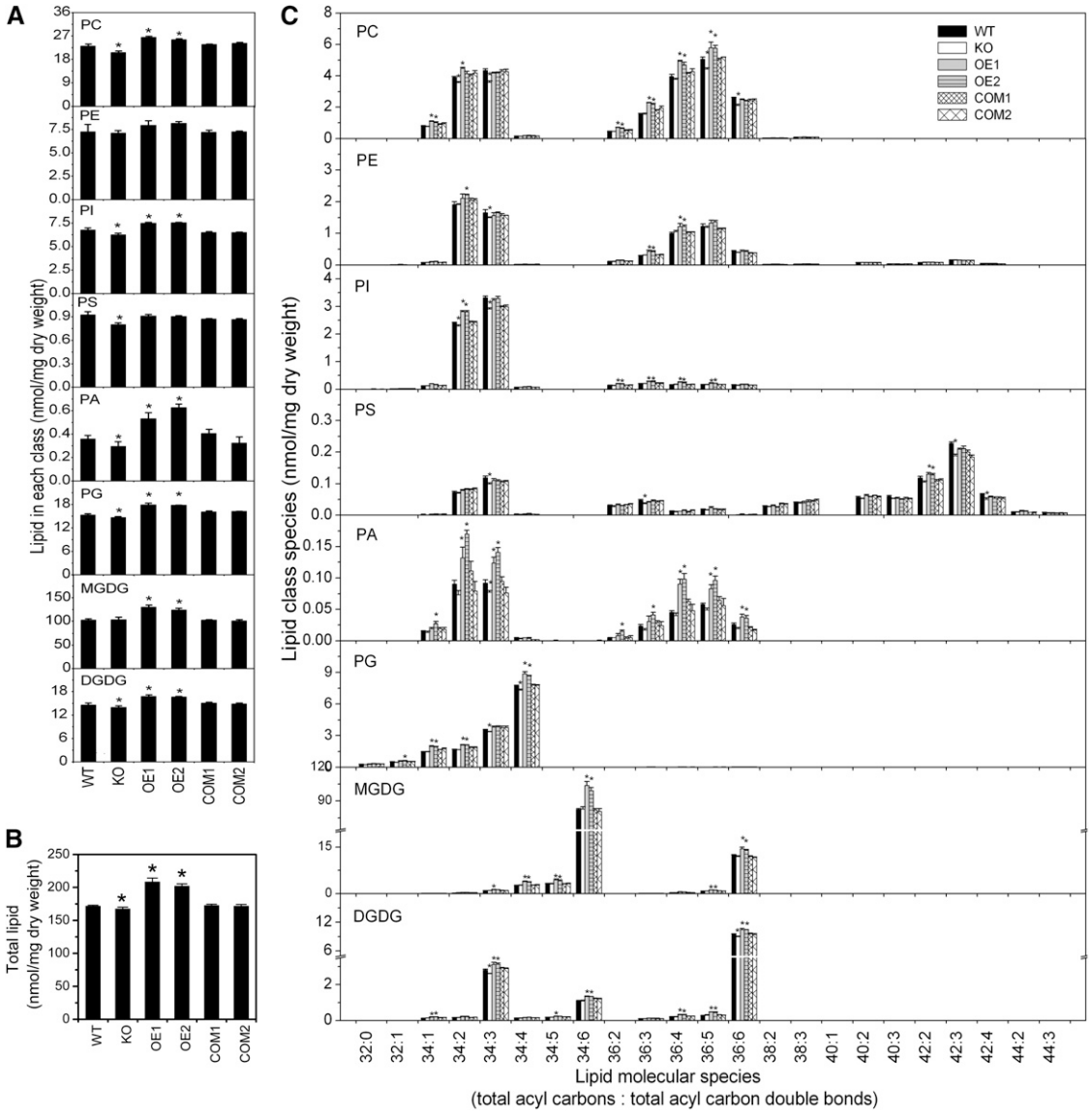

Figure 5. Effect of *pPLAIIIβ* Alterations on Phospholipid and Galactolipid Content in *Arabidopsis*.

Lipids from rosettes of 2-week-old soil-grown plants were quantified by ESI-MS/MS. Values are means ± SD ($n = 5$); each replicate contained at least three plant rosettes. Asterisk indicates significant difference at $P < 0.05$ compared with the wild type based on Student's *t* test.

(A) Phospholipid and galactolipid content of wild-type, KO, OE, and COM mutant rosettes. Phospholipids include PC, PE, PI, PS, PA, and PG; galactolipids include MGDG and DGDG.

(B) Total lipids in wild-type, KO, OE, and COM mutant lines. Total lipids refer to the total amount of PC, PE, PI, PS, PA, PG, MGDG, DGDG, LPC, LPE, and LPG.

(C) Molecular species of phospholipids and galactolipids in wild-type, KO, OE, and COM mutants. Phospholipids include PC, PE, PI, PS, PA, and PG; galactolipids include MGDG and DGDG.

flower buds were also shorter in OE than in the wild type (Figure 7E).

To determine the longitudinal growth in detail, the length of leaves, stalks, hypocotyls, and roots were measured (Figure 8A). The leaf blades and petioles of the fifth to eighth leaves of 5-week-old, soil-grown plants were longer in KO, but shorter in OE, mutants than in the wild type. However, the width of leaves was similar in wild-type, KO, and OE plants. Thus, the ratio of length to width was significantly greater in KO but smaller in OE compared with the wild type (Figure 8B). These data indicate that *pPLAIIIβ* inhibits longitudinal growth of leaves. The height of 8-week-old KO and wild-type plants was similar, but OE plants were 35% shorter than the wild type (Figure 8C). On the other hand, the diameters of the stems were ~33% wider in OE than

the wild type (Figure 8C). All internodes of OE were significantly shorter than those of the wild type (Figure 8C). Compared with the wild type, primary roots and hypocotyls were longer in KO, but shorter in OE (Figures 8D, 8F, and 8G); root hairs were also longer in KO but shorter in OE plants (Figures 8E and 8H). Genetic complementation of the KO mutant with *pPLAIIIβ* (COM) restored growth to the wild-type phenotype (Figures 8F and 8G), confirming that the root and hypocotyl growth alterations result from loss of *pPLAIIIβ*. Collectively, these data indicate that *pPLAIIIβ* impacts the longitudinal growth of plant organs.

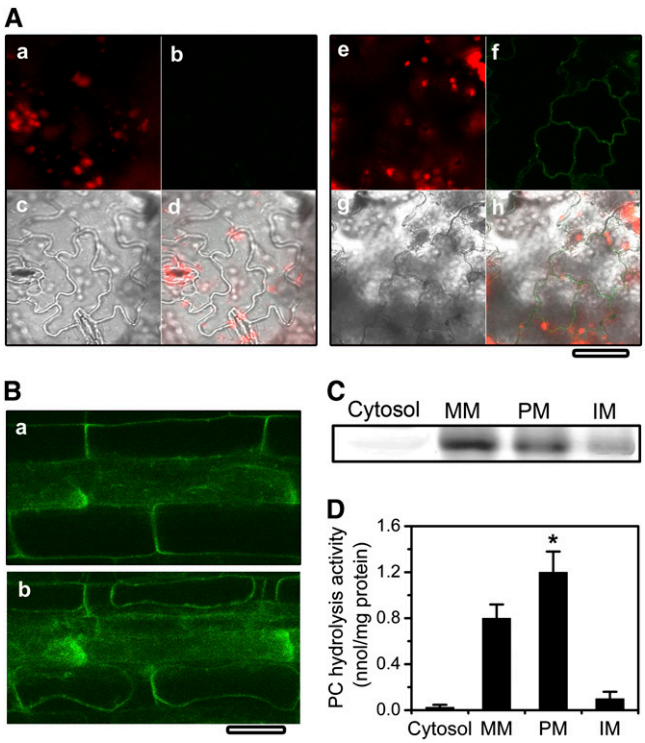

Figure 6. Subcellular Localization of pPLAIIIβ.

(A) Confocal micrographs of epidermal cells of wild-type leaf (**[a]** to **[d]**) and *pPLAIIIβ*-OE:GFP leaf (**[e]** to **[h]**) and chlorophyll fluorescence (**[a]** and **[e]**; red) versus GFP (**[b]** and **[f]**; green). The green fluorescent signal of GFP-tagged pPLAIIIβ is shown in **(f)**. Transmitted light (**[c]** and **[g]**) overlays (**[d]** and **[h]**) clarify cell outlines. Bar = 50 μm.
(B) Plasmolysis of root epidermal cells of the *pPLAIIIβ*-OE:GFP mutant. **(a)** Before plasmolysis: signal was at the cell surface; **(b)** 5 min after plasmolysis: signal was plasmolyzed. Bar = 50 μm.
(C) Subcellular fractionation of pPLAIIIβ. Twenty micrograms of soluble protein was loaded per lane, and 5 μg of protein was loaded per lane for membrane fractions. Cytosol, soluble fraction; MM, microsomal membrane fraction; PM, plasma membrane; IM, intracellular membrane.
(D) PC-hydrolyzing activity in pPLAIIIβ-OE membrane fractions from leaves. The same amounts of protein from the membrane fractions from wild-type leaves and pPLAIIIβ-OE leaves were used for the PLA assay. The pPLA activity due to overexpression of pPLAIIIβ is represented as the activity in the *pPLAIIIβ*-OE fraction minus the activity in the corresponding wild-type fraction ($n = 3$). Asterisk indicates significant difference at $P < 0.05$ compared with the cytosol, based on Student's *t* test.

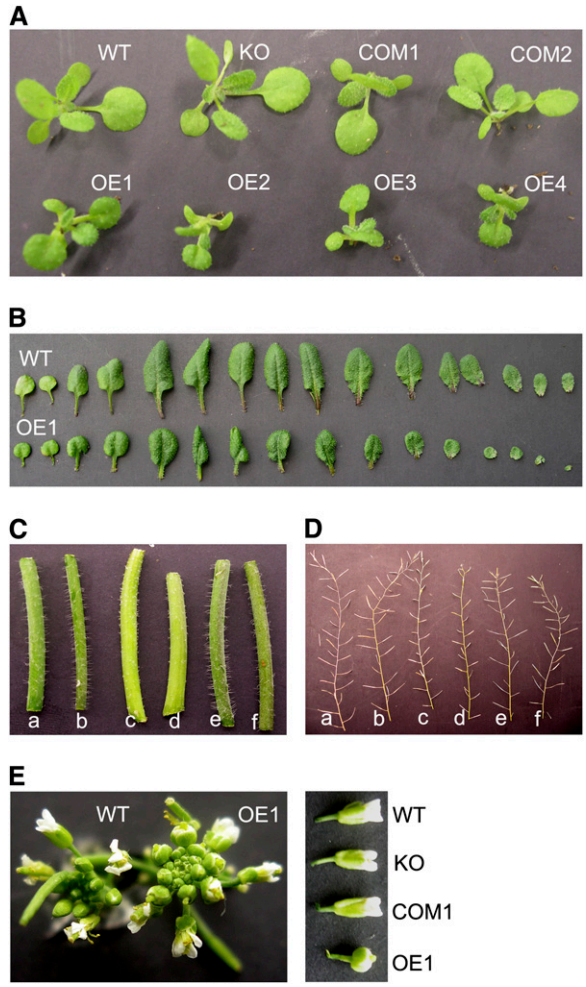

Figure 7. Altered Plant Size of Knockout and Overexpression Mutants of *pPLAIIIβ*.

(A) Morphology of 2-week-old plants. *pPLAIIIβ* knockout leads to slightly enlarged *Arabidopsis* plants, and overexpression of *pPLAIIIβ* leads to significantly smaller plants. The rosette leaves of OE plants are more compact than those of wild-type (WT) plants. KO, T-DNA insertion line; COM1, complementation line 1; COM2, complementation line 2; OE1 to 4, independent overexpression lines 1 to 4.
(B) Individual leaves of 4-week-old plants. The lengths of both blades and petioles in OE1 plants are reduced compared with those of the wild-type plants. From left to right, the leaves are arranged from cotyledons to the youngest leaves.
(C) Morphology of main inflorescence stalks of 8-week-old plants. The stalk of the OE plants is much thicker than that of a wild-type plant.
(D) Siliques of 8-week-old plants. The length of siliques and pedicels in OE plants are shorter than those of wild-type plants. In **(C)** and **(D)**, (a), wild type; (b), KO; (c), OE1; (d), OE2; (e), COM1; (f), COM2.
(E) Morphology of flowers. The length of flower buds in OE plants is shorter than in wild-type plants.
[See online article for color version of this figure.]

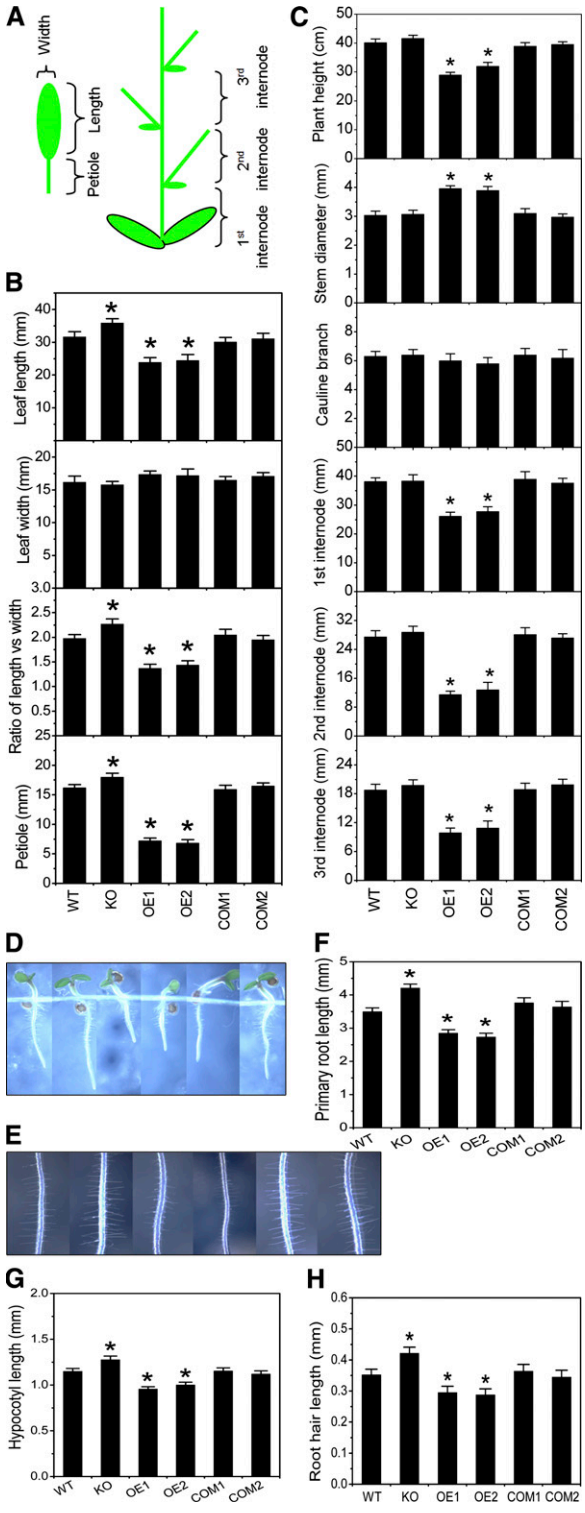

Figure 8. Altered Organ Length of Leaves, Stalks, Hypocotyls, Primary Roots, and Root Hairs of Knockout and Overexpression Mutants of *pPLAIIIβ*.

(A) Diagram showing the growth parameters measured, including leaf length, leaf width, petiole length, plant height, and length of 1st, 2nd, and 3rd internodes.

(B) The length and width of leaves. The fifth to eighth leaves of 5-week-old plants were measured. Lengths of leaf blades and petioles are slightly longer in KO and dramatically shorter in OE plants compared with wild-type leaves. Data are means ± SE of 20 leaves. Asterisk indicates significant difference at $P < 0.05$ compared with the wild type, based on Student's *t* test.

(C) Measurement of the length and width of main inflorescence stalks. The internodes of 8-week-old plants were measured. The main inflorescence of OE plants is shorter than that of wild-type plants and so is the length of the 1st, 2nd, and 3rd internodes. Data are means ± SE of 20 samples. Asterisk indicates significant difference at $P < 0.05$ compared with the wild type, based on Student's *t* test.

(D) Three-day-old seedlings of wild-type, KO, OE, and COM plants showing longer primary roots in KO plants and shorter ones in OE plants compared with the wild type and COM. Seedlings were grown in half-strength Murashige and Skoog agar medium plates in a horizontal orientation for 3 d, and growth parameters were measured.

(E) Root hairs of wild-type, KO, OE, and COM plants, showing increased and reduced length of root hairs in KO and OE plants, respectively, compared with the wild type.

(F) Primary root length in wild-type, KO, OE, and COM plants showing that KO has longer and OE has shorter primary roots in 3-d-old seedlings compared with wild-type and COM plants. Data are means ± SE of 20 samples. Asterisk indicates significant difference at $P < 0.05$ compared with the wild type based on Student's *t* test.

(G) Hypocotyl length in wild-type, KO, OE, and COM plants showing that KO has longer and OE has shorter hypocotyls in 3-d-old seedlings compared with the wild type and COM. Data are means ± SE of 20 samples. Asterisk indicates significant difference at $P < 0.05$ compared with the wild type based on Student's *t* test.

(H) Root hair length in the primary roots of wild-type, KO, OE, and COM plants showing that KO has longer and OE has shorter root hairs in 3-d-old seedlings compared with the wild type. Data are means ± SE of 50 samples. Asterisk indicates significant difference at $P < 0.05$ compared with the wild type based on Student's *t* test.

[See online article for color version of this figure.]

pPLAIIIβ Affects Anisotropic Cell Expansion and Elongation

To characterize the effect of *pPLAIIIβ* on longitudinal growth, the lengths of cells in the epidermis of leaves and of hypocotyls were measured. Pavement cells in the leaf epidermis were ~10% longer in KO but 20% shorter in OE than in the wild type, while the cells were slightly wider in OE than in the wild type and KO (Figures 9A to 9C). Similarly, epidermal cells in the middle part of hypocotyls were longer in KO but shorter in OE than those in the wild type, but the cells were >40% wider in OE than in the wild type (Figures 9D to 9F). Cells in the top and bottom parts of hypocotyls were also markedly shorter in OE than in the wild type (see Supplemental Figure 4 online). In addition, trichome cell branches were ~15% longer in KO but 35% shorter in OE, while the branches were generally wider in OE than in the wild type (Figures 9G and 9H).

In addition, leaf pavement cells had a less convoluted shape in OE and the lobes of pavement cells were shorter in KO than in the wild type (Figure 9A). In all tissues examined, cell number was similar in wild-type, KO, and OE plants (see Supplemental Figure 4B online), indicating that *pPLAIIIβ* does not affect cell division. The shorter and wider cells in *pPLAIIIβ*-OE tissues suggest that

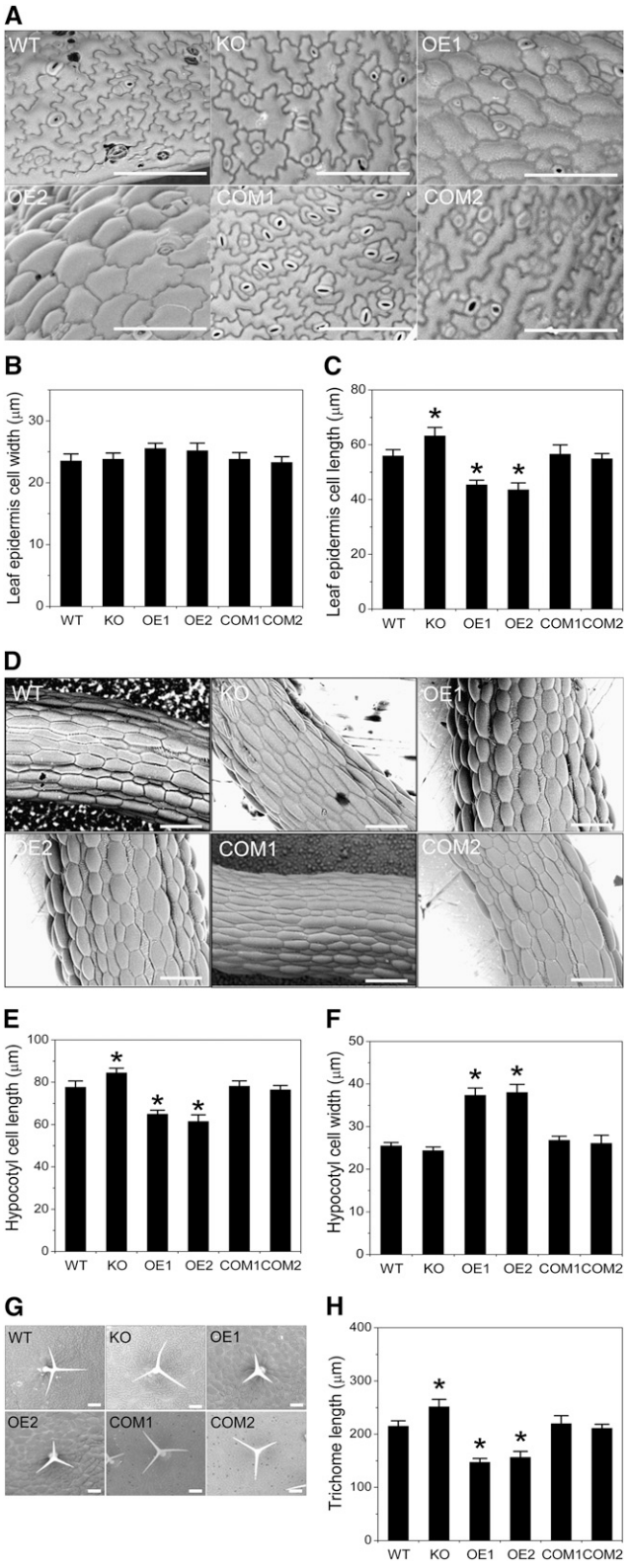

Figure 9. Altered Cell Length of Leaves, Trichomes, and Hypocotyls of Knockout and Overexpression Mutants of *pPLAIIIβ* Examined by Scanning Electron Microscopy.

Data are means ± SE of 20 samples and asterisk indicates significant difference at $P < 0.05$ compared with the wild type (WT), based on Student's *t* test (**[B]**, **[C]**, **[E]**, **[F]**, and **[H]**).

(A) Leaf epidermal cells of wild-type, KO, OE, and COM plants showing reduced cell length and reduced convolution of epidermal cells in OE plants compared with wild type. Bars = 100 μm.

(B) Leaf epidermal cell width showing little change in KO and OE plants compared with that of the wild type.

(C) Leaf epidermal cell length showing increased and reduced length in KO and OE plants, respectively, compared with the wild type. Seedlings were grown on half-strength Murashige and Skoog vertical plates for 3 d.

(D) Hypocotyl epidermal cells of wild-type, KO, OE, and COM plants showing reduced cell length in the OE plants. Bars = 100 μm.

(E) Hypocotyl cell length showing increased and reduced length in KO and OE plants, respectively, compared with the wild type. Seedlings were grown on half-strength Murashige and Skoog vertical plates for 3 d.

(F) Hypocotyl cell width showing no change in KO but an increase in OE plants compared with wild-type hypocotyl cell widths.

(G) Morphology of trichomes of wild-type, KO, OE, and COM plants showing slightly longer trichome branches in KO and shorter trichome branches in OE plants compared with those of the wild type. Bar = 100 μm.

(H) Length of trichome branches showing a slight increase in KO but a reduction in OE compared with the wild type.

pPLAIIIβ-OE is defective in control of cell anisotropic expansion, thus decreasing longitudinal growth.

pPLAIIIβ Decreases Mechanical Strength and Cellulose Content

During handling of the OE plants, we noticed that the leaves and stalks were brittle. When the main inflorescence stalk was bent at a 90°C angle, wild-type stalks were flexible but OE stalks often broke (Figure 10A). The fragility was also observed for the branches of the stalk in OE (Figure 10B). Compared with the wild type, the force required to break the stalk of the main inflorescence was ~10% greater for KO but 50% less for OE (Figure 10C).

The mechanical strength of a stalk is related to properties of the cell wall and the length and strength of fiber cells (Mauseth, 1988). Cellulose is an important component of the cell wall that is associated with mechanical strength. Thus, we measured the levels of cellulose in wild-type, KO, OE, and COM plant stalks. The cellulose content was 10% higher in KO but 40% lower in OE than in the wild type (Figure 10D). Therefore, the decreased mechanical strength of the OE stalk may result, in part, from decreased content of cellulose.

The structure of interfascicular fiber cells was examined in cross sections and longitudinal sections of stalks. The stalk cells, including cortex, epidermis, pith, and xylem cells, were generally wider in OE than in the wild type (Figures 11A and 11B). The increased cell width was consistent with the increased stalk width in OE being due to cell width rather than cell number changes. The fiber cell wall was thinner in OE than in the wild type (Figures 11C and 11D). In addition, the length of interfascicular fiber cells was shorter in OE than in the wild type (Figures 11E and 11F). Collectively, the data suggest that overexpression of

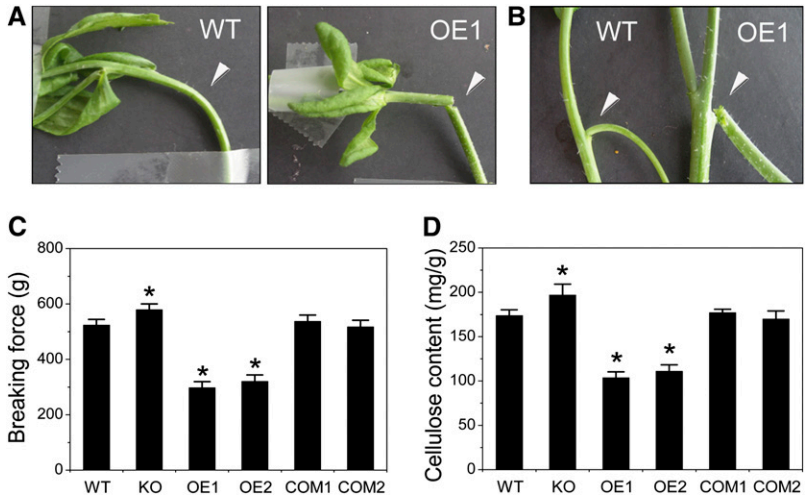

Figure 10. Altered Mechanical Strength and Cellulose Content in Knockout and Overexpression Mutants of *pPLAIIIβ*.

(A) Physical properties of main inflorescence stalks of wild-type (WT) and OE1 plants showing an easily broken stalk, as indicated by the arrow.
(B) Physical properties of branching stalks of wild-type and OE1 plants showing an easily broken branching stalk, as indicated by the arrow.
(C) Measurement of the force required to break the main inflorescence stalks in the bottom segment, showing that the mechanical strength was slightly increased in KO and dramatically reduced in OE stalks. Breaking force is defined as the gram of weight needed to break the stem. Data are the mean values ± SE for the bottom stalk segment of 20 plants. Asterisk indicates significant difference at $P < 0.05$ compared with the wild type based on Student's *t* test.
(D) Measurement of the cellulose content of wild-type, KO, OE, and COM plant stalks showing slightly increased but dramatically reduced cellulose content in KO and OE stalks, respectively, when compared with the wild type. Data are means ± SE of 10 samples. Asterisk indicates significant difference at $P < 0.05$ compared with the wild type based on Student's *t* test.
[See online article for color version of this figure.]

pPLAIIIβ decreases plant mechanical strength due to decreased levels of cellulose; the decreased cellulose level may result in thinner cell walls, as well as the shorter fiber cells in OE plants.

pPLAIIIβ-Altered Seedlings Respond Differently to FFAs That Inhibit Root Elongation

We tested the effect of FFAs, the direct reaction products of pPLAIIIβ, on cell elongation in primary roots. The most abundant FFA in *Arabidopsis*, 18:3, was tested first. When 3-d-old seedlings were transferred to a plate containing 50 μM 18:3, primary root elongation was inhibited in a concentration-dependent manner in all genotypes (Figures 12A and 12B). However, the KO roots were less sensitive and OE more sensitive than wild-type roots (Figure 12B). The IC_{50} of 18:3 was ~25 μM for OE roots, but 50 μM for KO roots. At 50 μM 18:3, root elongation was inhibited by ~50% in KO, 60% in the wild type, and 70% in OE plants. Treatment with 50 μM 18:3 had a greater effect on decreasing cell length (see Supplemental Figures 5A and 5B online) than cell width or cell number (see Supplemental Figures 5C and 5D online). When different FFA species were examined, saturated 16:0 and 18:0 had no detectable effects on root elongation at the concentrations examined. All unsaturated 18 carbon species inhibited root elongation, and the degree of inhibition was 18:3>18:2>18:1 (Figure 12C).

Another reaction product of pPLAIIIβ is lysophospholipids, and their levels were increased in OE plants (Figure 4E). Both LPC and lysophosphatidylethanolamine (LPE) inhibited root elongation, and at 1 μM, root length was 40% shorter than roots grown in the absence of lysophospholipids. Wild-type, KO, and OE plants responded similarly to LPC or LPE (Figures 12D and 12E).

α-Linolenic acid (18:3) was the most effective FFA tested on root growth inhibition. 18:3 can be readily converted to oxylipins, such as OPDA, JA, and JA-Ile. Since JA is known to cause inhibition of root growth, we tested whether *pPLAIIIβ* mutant plants had altered JA levels. Oxylipins, OPDA, JA, and JA-Ile were measured in plate-grown OE, wild-type, and KO plants. OE plants had significantly higher levels of oxylipins than KO plants (Figure 12F). KO plants tended to have less oxylipins, whereas OE plants had more oxylipins than the wild type, but neither OE nor KO was significantly different from the wild type (Figure 12F).

DISCUSSION

The results of this study show that pPLAIIIβ possesses acyl-hydrolyzing activity. Unlike pPLAI and the pPLAIIs, pPLAIIIs do not have a conserved *S-D* dyad and lack the canonical esterase box *GxSxG* or the conserved *DGG* motif. An esterase (EstA) secreted by the plant pathogen *Streptomyces scabies* lacks the *GxSxG* motif but hydrolyzes ester bonds in plant suberin (Raymer et al., 1990). The deduced SAG101 protein with a *GxSxA* (not *GxSxG*) in the N-terminal conserved regions also possesses acyl hydrolase activity toward triacylglycerol (He and Gan, 2002). On

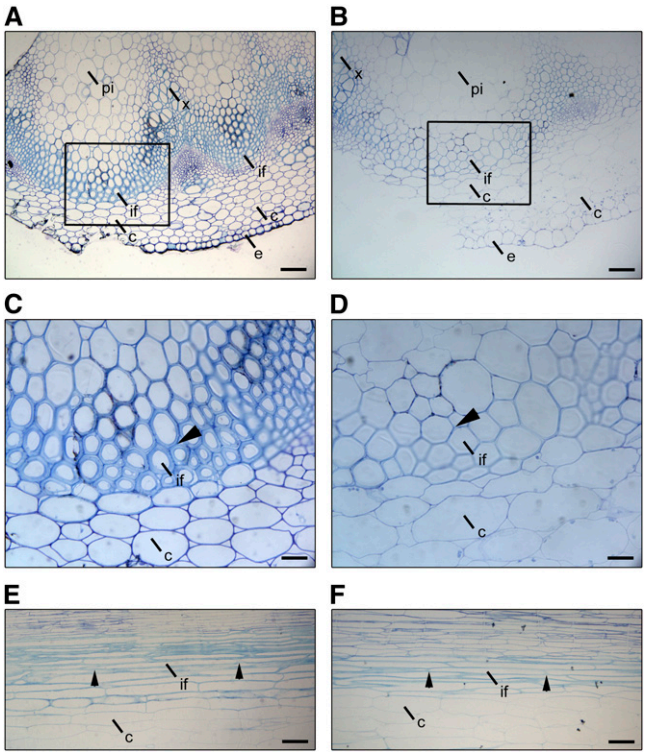

Figure 11. Altered Anatomy of Interfascicular Fibers in Stalks of Overexpression Mutants of *pPLAIIIβ* Compared with Those of the Wild Type.

(A) to **(D)** Transverse sections of the stalks of 8-week-old wild-type **(A)** and OE1 plants **(B)** stained with toluidine blue showing differences in interfascicular fibers (if).

(C) and **(D)** Enlargement of the boxed regions indicated in **(A)** and **(B)** showing that the fiber cell wall (arrows) in the wild type **(C)** is thicker than that in OE1 **(D)**.

(E) and **(F)** Longitudinal sections of the stalk of wild-type **(E)** and OE1 plants **(F)**. Fiber cells in OE1 are shorter and wider than those in the wild type. Arrows mark the ends of a fiber cell. c, cortex; e, epidermis; if, interfascicular fiber; pi, pith; x, xylem.

[See online article for color version of this figure.]

the other hand, some Ser hydrolases with esterase activity also contain a *GxSxG* motif but use nonlipid substrates (Ollis et al., 1992). Therefore, the *GxSxG* motif is typical of, but seems not to be essential for, lipid deacylating enzymes. Interestingly, pPLAIIIα and pPLAIIIδ have a second motif, *DGG*, which is conserved, suggesting that their catalytic site and mechanism of catalysis may differ even within the pPLAIII subfamily.

The finding that pPLAIIIβ has acyl-CoA thioesterase activity raises further questions about the metabolic function of this enzyme. Multiple acyl-CoA thioesterases have been reported in animals and bacteria and are grouped based on their intracellular association (cytosolic, mitochondrial, or peroxisomal) and sequence similarity. However, the physiological roles of acyl-CoA thioesterases remain unclear. One role suggested for peroxisomal acyl-CoA thioesterases is in fatty acid oxidation (Tilton et al., 2004). Information on plant acyl-CoA thioesterases is limited. One *Arabidopsis* peroxisomal acyl-CoA thioesterase, ACH2, has been cloned and biochemically characterized, and the data suggest that this enzyme is unlikely to be involved in fatty acid oxidation, but its function is unclear (Tilton et al., 2004). A thioesterase activity was previously reported for mammalian $iPLA_2\beta$, which is also a patatin domain-containing enzyme (Jenkins et al., 2006). However, unlike plant pPLAIIIβ, $iPLA_2\beta$ possesses the canonical G*x*S*x*G lipase consensus sequence motif, and both the PLA_2 and thioesterase activities of $iPLA_2\beta$ use the same active site and the nucleophile Ser-465. pPLAIIIβ contains no S-D dyad; thus, the catalytic sites for the thioesterase and for PLA activities remain to be determined. It is possible that other pPLA members may also have acyl-CoA thioesterase activity. Since *Arabidopsis* pPLAIIIβ is associated with the plasma membrane, its function is not related to peroxisomal oxidation of fatty acids. Interestingly, some acyl-CoA binding proteins are also associated with the plasma membrane (Gao et al., 2010). Acyl-CoA binding protein 2 binds LPC and lysophospholipase 2 (Gao et al., 2010), both of which act downstream of pPLAIII. These findings could mean the presence of a plasma membrane–based metabolic complex that uses acyl-CoA. The metabolic and physiological functions of proteins interacting with acyl-CoA in the plasma membrane remain to be elucidated.

pPLAIIIβ-KO has a lower level, whereas *pPLAIIIβ*-OE has a higher level of FFAs than the wild type, and these opposite effects on FFAs in KO and OE are intuitive, providing in planta evidence for the function of the enzyme. Likewise, the increases of LPC, LPE, and lysophosphatidylglycerol (LPG) in the OE plants also provide evidence for increased activity of the enzyme in planta. On the other hand, the KO plants have a comparable level of lysophospholipids as the wild type, even though some lysophospholipid species tend to be lower than in the wild type. This metabolic phenotype is consistent with morphological changes exhibited by the KO and OE plants. The lack of an overt decrease of lysophospholipids in the KO could result from partially redundant functions of other *pPLAIII*s. Specifically, *pPLAIIIα* and *pPLAIIIβ* display some overlapping expression patterns.

The levels of total membrane glycerolipids tended to be lower in the rosettes of *pPLAIIIβ*-KO and higher in those of *pPLAIIIβ*-OE than in those of the wild type. The result is counterintuitive, considering that pPLAIIIβ hydrolyzes phospholipids and galactolipids in vitro. One interpretation is that the overexpression of *pPLAIIIβ* may accelerate lipid biosynthesis (Figure 13). pPLAIIIβ is mostly associated with the plasma membrane, whereas PC and PE, the substrates of pPLAIIIβ, are the predominant glycerolipids. LPC and LPE can be acylated to form PC and PE. Deacylation and reacylation may be involved in lipid remodeling and might accelerate the lipid biosynthesis flux by acyl editing. The increased ratio of lipids containing 36 carbons in acyl chains over lipids with 34 carbons in OE compared with wild-type plants in PC, PE, phosphatidylinositol (PI), PS, PA, and PG is consistent with the idea that the initially formed 34-carbon (16C/18C combinations) phospholipids may be more actively remodeled in the OE plants by adding longer acyl chains (see Supplemental Figure 6 online). In *Arabidopsis*, 34C diacyl polar lipids are 16C/18C combinations, while 36C species are di18C combinations (Devaiah et al., 2006).

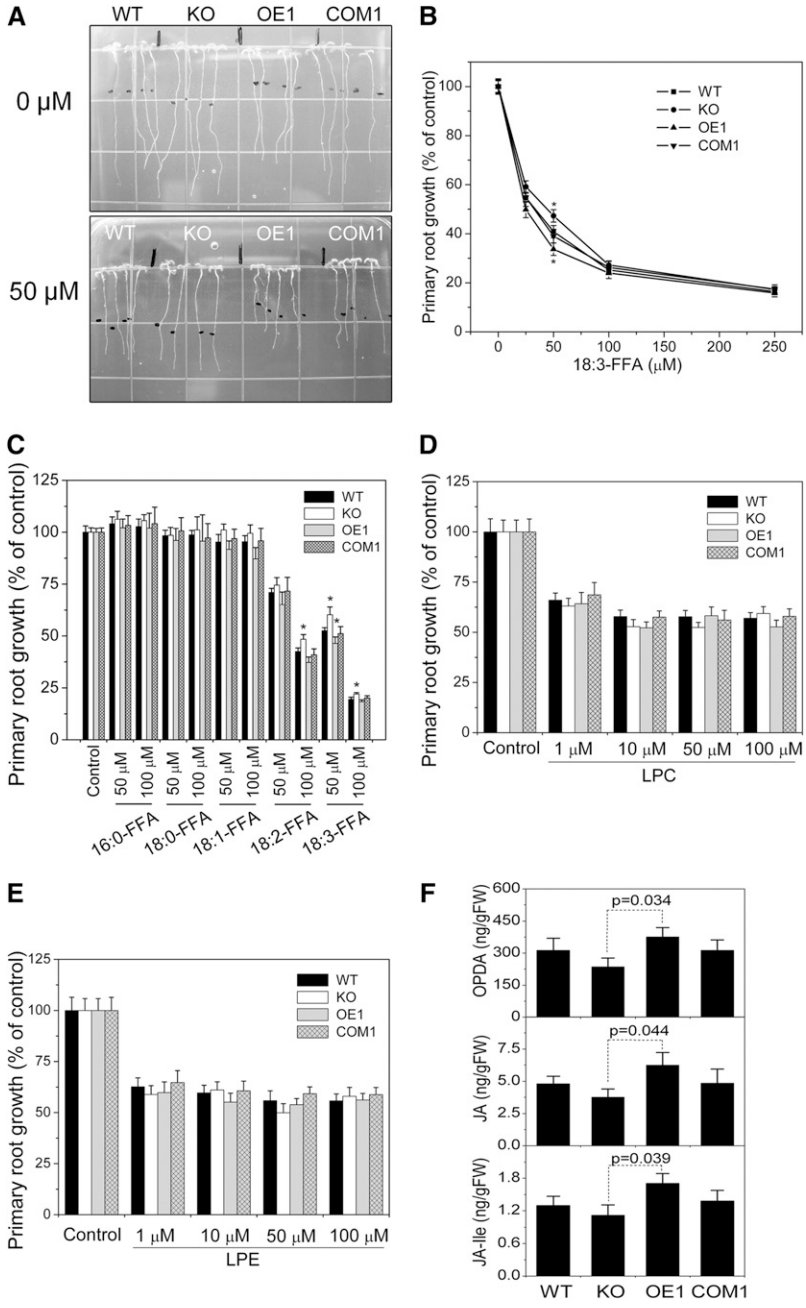

Figure 12. Altered Sensitivity of Plant Root Growth of KO and OE1 in Response to Treatment by FFA but Not Lysophospholipids.

(A) Root growth inhibition by FFA (18:3-FFA) showing that primary root growth of KO is less sensitive and OE1 is more sensitive to 50 μM 18:3 (FFA) treatment compared with the wild type (WT). Three-day-old seedlings grown on half-strength Murashige and Skoog plates were transferred to new plates containing the indicated concentrations of FFA for 2 d. The arrows mark the newly emerged primary root after 2 d.

(B) Response of primary root growth to various concentrations of 18:3, showing that the OE1 plant has more and the KO plant has less sensitivity to the treatment compared with the wild type. The difference is particularly significant with the 50 μM 18:3 treatment. Values are means ± SE (n = 18). Asterisk indicates significant difference at $P < 0.05$ compared with the wild type based on Student's t test.

(C) Response of primary root growth to various types of FFA in wild-type, KO, OE1, and COM1 plants. Three-day-old seedlings were transferred to new plates containing the indicated amount of FFA. After 2 d, the newly elongated primary root length was measured. The root growth in the control plate was set as 100%. Five types of FFAs were applied: 16:0, 18:0, 18:1, 18:2, and 18:3. Data are means ± SE of 18 samples. Asterisk indicates significant difference at $P < 0.05$ compared with the wild type based on Student's t test.

(D) Response of primary root growth to various concentrations of LPC, showing little difference in wild-type, KO, OE1, and COM1 plant response. Data are means ± SE of 18 samples.

Analysis of *pPLAIIIβ*-altered plants indicates that *pPLAIIIβ* impedes anisotropic cell expansion but not cell division. OE plants had shorter and wider cells, whereas KO plants had longer cells than the wild type. The effect may have resulted, at least in part, from elevated intracellular levels of FFAs in *pPLAIIIβ*-OE *Arabidopsis* plants. We tested the effect of FFAs on root growth and cell length and found that unsaturated 18 carbon fatty acids inhibited root elongation. Furthermore, *pPLAIIIβ*-OE seedlings were more sensitive than wild-type seedlings to unsaturated FFAs, whereas KO seedlings were less sensitive. The increased sensitivity may be due to the already elevated intracellular levels of FFAs in the OE seedlings and reduced levels of FFAs in KO plants. Thus, it took a lower level of FFAs in OE than the wild type or KO to reach the same threshold of inhibition of growth. FFAs have been reported as inhibitors of tobacco (*Nicotiana tabacum*) auxillary bud growth (Tso, 1964), buckwheat (*Fagopyrum esculentum*) seedling growth (Tsuzuki et al., 1987), straight growth of the *Avena* coleoptile (Ohkawa and Nishikawa, 1987), and growth of the microalgae *Monodus subterraneus* (Bosma et al., 2008). In addition, lysophospholipids also inhibit cell and root elongation. A combination of effects resulting from the elevated FFAs and lysophospholipids may result in shorter cells and plants.

The mechanism whereby FFAs and lysophospholipids inhibit anisotropic cell expansion and cell elongation is unclear. We explored the possibility that the increase in FFAs, particularly in free linolenic acid, may increase oxylipin production, as 18:3 may serve as a substrate for JA biosynthesis. JA is known to inhibit root growth. However, the level of JA and JA-Ile is not significantly higher in OE than in wild-type plants. In addition, other fatty acids, such as 18:1 and 18:2, which are not substrates for JA, also inhibit root elongation. These results suggest that it is unlikely that FFAs inhibit cell elongation due to their conversion to oxylipins.

The dramatic reduction in cellulose content in *pPLAIIIβ*-OE plants may provide an explanation for the defects in anisotropic cell expansion and decreased longitudinal growth. The stalks of *pPLAIIIβ*-KO had a 40% reduction in cellulose content. Several cellulose-deficient mutants, such as *csi1* (cellulose synthase-interactive protein 1) and *ctl1*/*pom1*, display similar defects in the regulation of anisotropic expansion and cell elongation phenotypes (Zhong et al., 2002; Gu et al., 2010). Cell wall production is regarded as a driving force for cell expansion, and the direction of expansion is regulated in part by the oriented deposition of cellulose microfibrils around the cell.

This raises an intriguing question as to how increased *pPLAIIIβ* expression decreases cellulose production. The changed membrane lipid composition, particularly elevated levels of FFAs from pPLAIIIβ-hydrolyzing activity, may inhibit cellulose biosynthesis, deposition, or both (Figure 13). It has been reported that unsaturated FFA inhibits the H^+/K^+-ATPase but that saturated FFAs do not (Swarts et al., 1991). Similarly, FFAs are known to inhibit Na^+/K^+-ATPase and to a greater extent as the number of double bonds increases (Lamers and Hülsmann, 1977; Swann, 1984). FRA2, an AAA-ATPase, is responsible for cellulose deposition in *Arabidopsis* stalks; loss of function of *FRA2* results in decreased cellulose content and decreased mechanical strength (Burk et al., 2001). pPLAIIIβ is localized at the plasma membrane; increasing its expression may elevate the level of FFAs and inhibit the ATPase activity of FRA2 in the plasma membrane in *pPLAIIIβ*-OE plants.

In summary, we have shown that pPLAIIIβ, which lacks the canonical esterase catalytic center, possesses acyl-hydrolyzing and thioesterase activities. Alteration of *pPLAIIIβ* expression

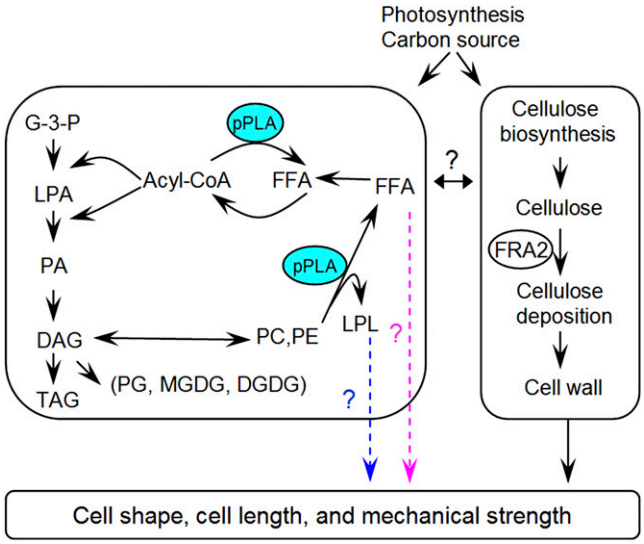

Figure 13. A Working Model of the Effects of pPLAIIIβ on Lipid Metabolism, Cellulose Content, Cell Elongation, Cell Morphology, and Mechanical Strength.

pPLAIIIβ hydrolyzes acyl-CoA and phospholipids such as PC and generates FFA and lysophospholipids, such as LPC. The released FFA and lysophospholipids can be reacylated. The hydrolysis catalyzed by pPLAIIIβ may facilitate the lipid metabolic flux and results in the increased synthesis of other phospholipids, such as PC, PE, PG, and PA, and galactolipids, such as MGDG and DGDG. As a result, less carbon from photosynthesis may be partitioned into the synthesis of cellulose for cell wall synthesis, which provides the plant with mechanical strength. DAG, diacylglycerol; FRA2, fragile fiber 2; G-3-P, glycerol-3-phosphate; LPA, lysophosphatidic acid; lysoPL, lysophospholipids; TAG, triacylglycerol.

[See online article for color version of this figure.]

Figure 12. (continued).

(E) Response of primary root growth to various concentrations of LPE showing little difference in wild-type, KO, OE1, and COM1 plant response. Data are means ± SE of 18 samples.

(F) Oxylipin levels in wild-type, KO, OE1, and COM1 plant seedlings showing a significant difference between KO and OE1 seedlings. Five-day-old seedlings grown on half-strength Murashige and Skoog plates were harvested for oxylipin measurements. Values are means ± SE ($n = 5$). Inset: P value based on Student's *t* test. FW, fresh weight.

impacts lipid levels, cellulose content, and cell elongation. Our data suggest possible connections among lipid metabolism, cellulose production, and anisotropic cell growth (Figure 13). The precise role of lipid metabolism and signaling in the regulation of cellulose content and anisotropic cell growth warrants further investigation.

METHODS

pPLAIIIβ Cloning and Protein Purification from *Escherichia coli*

The full-length cDNA of *pPLAIIIβ* was obtained by PCR using an *Arabidopsis thaliana* cDNA library as a template and a pair of primers: forward 5′-TCAGGATCCATGCATAGAGTACGCAATAAACCGG-3′ and reverse 5′-CTTGTCGACTCGTTCTCTTGCGGTCACACC-3′. The cDNA was cloned into the pET28a vector before the 6xHis coding sequence. The 6xHis fusion construct was sequenced and confirmed to be error-free before it was introduced into *E. coli* strain Rosetta (DE3) (Amersham Biosciences). The bacteria were grown to an OD_{600} of 0.7 and induced with 0.1 mM isopropyl 1-thio-β-D-galactopyranoside for 16 h at 16°C. The pPLAIIIβ-His fusion protein was purified as described previously (Pappan et al., 2004). Briefly, the bacterial pellet was resuspended in STE buffer containing 1 mg/mL lysozyme (50 mM Tris-HCl, pH 8.0, 150 mM NaCl, and 1 mM EDTA). The samples were kept on ice for 30 min. DTT and *N*-laurylsarcosine (Sarkosyl) were added to a final concentration of 5 mM and 1.5% (w/v), respectively. The suspension was vortexed and sonicated on ice for 5 min. After centrifugation at 10,000*g* for 20 min, the supernatant was transferred to a new tube. Triton X-100 was added to a final concentration of 4% (v/v) and 6xHis agarose beads were added (10%, w/v). The solution was gently rotated at 25°C for 1 h. The fusion proteins bound to agarose beads were washed with 20 volumes of STE buffer. The amount of purified protein was measured with a protein assay kit (Bio-Rad).

Overexpression and Purification of pPLAIIIβ in *Arabidopsis*

The genomic sequence of *pPLAIIIβ* was obtained by PCR using Col-0 *Arabidopsis* genomic DNA as a template and primers of forward 5′-ATTTAATTAAATGCATAGAGTACGCAATAAACCG-3′ and reverse 5′-ATG-GCGCGCCATCGTTCTCTTGCGGTCACACCG-3′. The genomic DNA was cloned into the pMDC83 vector before the GFP-His coding sequence (GFP-6x histidine). The expression of *pPLAIIIβ* was under the control of the 35S cauliflower mosaic virus promoter. The sequence of the fusion construct was verified before it was introduced into *Agrobacterium tumefaciens* strain C58C1. The wild-type plants (Col-0) were transformed with this construct; transgenic plants were screened and confirmed by PCR. Over 15 independent transgenic lines were obtained (*pPLAIIIβ-OE*) with similar plant stature. Lines 1 to 5 were further verified by immunoblotting with anti-GFP antibody. The pPLAIIIβ-GFP-His protein was purified from *pPLAIIIβ*-OE plant leaves using 6xHis agarose beads (Qiagen) with the same procedure as for protein purification from *E. coli*.

Enzyme Assays

Phospholipids and acyl-CoAs were purchased from Avanti Polar Lipids. Phosphatidylcholine molecular species were 16:0-18:2 PC and 16:0-18:1 PC. PE, PG, PS, and PA were all 16:0-18:1 species. Acyl-CoAs were 18:2-CoA and 18:3-CoA. Galactolipids were purchased from Matreya. MGDG is a mixture of 16:0-18:0 and 18:0-18:0 MGDG, and DGDG is a mixture of 16:0-18:0 and 18:0-18:0 DGDG. Lipids in chloroform were dried under a nitrogen stream and emulsified in reaction buffer (25 mM HEPES, pH 7.5, 10 mM $CaCl_2$, and 10 mM $MgCl_2$) by vortexing, followed by 5 min sonication under 40% energy output on ice. Acyl hydrolyzing activities were assayed in a reaction mixture containing 25 mM HEPES, pH 7.5, 10 mM $CaCl_2$, and 10 mM $MgCl_2$. Sixty micromole lipids was used as substrate. Ten micrograms of purified protein was added to the mixture in a final volume of 500 μL. The reaction samples were incubated at 30°C for 60 min, and the reaction was stopped by adding 2 mL of chloroform/methanol (2:1, v/v) and 500 μL 25 mM LiCl. After vortexing and separation by centrifugation, the lower phase was transferred to a new glass tube. The upper phase was extracted twice more by adding 1 mL of chloroform each time, and the three lower phases were combined. Lipid internal standards were added, and lipid quantification was performed by mass spectrometry as described below.

Lipid Profiling and Hormone Analysis

Lipids were extracted and analyzed by electrospray ionization–tandem mass spectrometry (ESI-MS/MS), and the levels of PA, PC, PE, PG, PI, PS, MGDG, and DGDG were determined as previously described (Welti et al., 2002) with modifications described by Xiao et al. (2010). FFAs were determined by ESI-MS, using the deuterated internal standard (7,7,8,8,-d4-16:0 fatty acid) (Sigma-Aldrich) by scanning in the negative ion mode in a mass range of *m/z* 200 to *m/z* 350. Acyl-CoAs in the in vitro reaction samples were determined by ESI-MS/MS in the neutral loss mode (NL 509) using internal standards of 17:0-CoA (heptadecanoyl CoA) and 14:0e-CoA (tetradecyl CoA) (Avanti Polar Lipids). Fatty acids and major components of cuticle wax, C29 alkane, and C29 ketone were extracted and measured (Li-Beisson, 2010; Rowland, 2010).

For hormone extraction, ~50 mg of fresh *Arabidopsis* seedlings was sealed in 1.5-mL snap-cap vials. After freezing in liquid nitrogen, the tissues were ground to powder, and 500 μL of 2-propanol/water/concentrated HCl (2:1:0.002, v/v/v), with dihydrojasmonic acid as an internal standard, was added, followed by agitation for 30 min at 4°C. One milliliter of dichloromethane was added, followed by agitation for another 30 min at 4°C. After centrifugation at 13,000*g* for 5 min, the bottom layer was used for analysis of JA, JA conjugate JA-Ile, and OPDA by a liquid chromatography-multiple reaction monitoring–tandem mass spectrometry method described previously (Pan et al., 2008, 2010; Pan and Wang, 2009).

Plant Growth and Treatment

Surface-sterilized seeds were germinated in half-strength Murashige and Skoog salt agar for 3 d and then transferred to new plates with the indicated concentrations of FFA or lysophospholipids. After two more days of growth on vertical plates, the total length, cell length, and cell width of the newly elongated primary root were measured. Seedlings were grown on plates in a vertical orientation in a growth room with a 16-h-light/8-h-dark cycle, and at 23/21°C, under cool fluorescent white light (200 μmol m^{-2} s^{-1}). For experiments on soil-grown plants, plants were grown in growth chambers with a 12-h-light/12-h-dark cycle, at 23/21°C, 50% humidity, at 200 μmol m^{-2} s^{-1} of light intensity, and watered with fertilizer once a week.

Generation of Knockout and Overexpression Mutants and Complementation

A *pPLAIIIβ* T-DNA insertion mutant was identified from Salk_057212 of the Salk *Arabidopsis* T-DNA knockout collection from the Ohio State University ABRC. The homozygous T-DNA insertion mutant *pPLAIIIβ*-KO was isolated by PCR-based screening using two *pPLAIIIβ*-specific primers (5′-TTGACGGATATGCAGGAACCAA-3′ and 5′-ATGCGTGATTGCAGCC-GCTGT-3′) and a T-DNA left border primer (5′-GCGTGGACCGCTTGCTG-CAACT-3′). The loss of transcription of *pPLAIIIβ* was confirmed by real-time PCR. To generate the complementation lines, the genomic sequence of

pPLAIIIβ from the promoter region to the terminator region was cloned using two primers (5′-AGGCGCGCCCTAGCTCAATATGCAAA-3′ and 5′-AGGCGCGCCAAGTGGGATTTTATGAC-3′) and fused into a binary vector pEC291 for plant transformation.

Cellulose Measurement

Stalks were cut into pieces and ground into powder under liquid nitrogen. The materials were then extracted twice with 70% ethanol at 70°C for 1 h. Cell wall materials were dried under vacuum for cellulose content measurement (Updegraff, 1969). Whatman 3MM filter paper was used to establish a standard curve for quantification of cellulose. The anthrone reagent was used to determine the cellulose content.

RNA Extraction and Real-Time PCR

Real-time PCR was performed as described by Li et al. (2006). Briefly, total RNA was extracted from different tissues using the cetyl-trimethylammonium bromide method. DNA contamination in RNA samples was removed with RNase-free DNase. An iScript kit (Bio-Rad) was used to synthesize cDNA from isolated RNA template by reverse transcription. The MyiQ sequence detection system (Bio-Rad) was used to detect products during quantitative real-time PCR by monitoring SYBR green fluorescent labeling of double-stranded DNA. Efficiency was normalized to a control gene UBQ10 or *β-tubulin*. The data were expressed as mean ± SD (n = 3 technical replicates). The primers for *pPLAIIIβ* were 5′-TTCGAGAAGCTTGACTGGTTAGCTGG-3′ (forward) and 5′-TTTCATCGTTCTCTTGCGGTCACACC-3′ (reverse). The primers for *UBQ10* were 5′-CACACTCCACTTGGTCTTGCGT-3′ (forward) and 5′-TGGTCTTTCCGGTGAGAGTCTTCA-3′ (reverse). The primers for *β-tubulin* were 5′-GCCAATCCGGTGCTGGTAACA-3′ (forward) and 5′-CATACCAGATCCAGTTCCTCCTCCC-3′ (reverse). PCR conditions were as follows: one cycle of 95°C for 1 min; 40 cycles of DNA melting at 95°C for 30 s, DNA annealing at 55°C for 30 s, and DNA extension at 72°C for 30 s; and final extension of DNA at 72°C for 10 min.

Microscopy Imaging

For bright-field light microscopy, stalk sections were fixed in 2% glutaraldehyde in PBS (33 mM Na_2HPO_4, 1.8 mM NaH_2PO_4, and 140 mM NaCl, pH 7.3) at 4°C overnight. After fixation, segments were dehydrated through a graded ethanol series, rinsed in acetone, and embedded in Spurr's resin (Electron Microscopy Sciences). One-micrometer-thick sections were stained with toluidine blue for observation in a Nikon Eclipse 800 light microscope. For scanning electron microscopy, fresh samples were glued to specimen stubs using OCT, frozen in liquid nitrogen for 1 min, and then immediately transferred to the scanning electron microscope for observation in the frozen state using the backscatter detector of a Hitachi TM 1000 tabletop scanning electron microscope (Hitachi High-Technologies Canada). The subcellular location of GFP-tagged protein was determined using a Zeiss LSM 510 confocal microscope equipped with a ×40 differential interference contrast, 1.2–numerical aperture water immersion lens. Plasmolysis in primary root cells was induced by immersing roots in 0.5 M NaCl for 5 min.

Subcellular Fractionation

Proteins were extracted from leaves of 4-week-old plants using buffer (30 mM HEPES, pH 7.5, 400 mM NaCl, and 1 mM phenylmethanesulfonyl fluoride), followed by centrifugation at 6,000*g* for 10 min. The supernatant was centrifuged at 100,000*g* for 60 min. The resultant supernatant is referred to as the soluble cytosol fraction, and the pellet is referred to as the microsomal fraction. Using two-phase partitioning as described previously (Fan et al., 1999; Hong et al., 2009), the microsomal fraction was separated further into plasma membrane and intracellular membrane fractions.

Accession Numbers

Sequence data from this article can be found in the Arabidopsis Genome Initiative database under the following accession numbers: *pPLAI*, At1g61850; *pPLAIIα*, At2g26560; *pPLAIIβ*, At4g37050; *pPLAIIγ*, At4g37070; *pPLAIIδ*, At4g37060; *pPLAIIε*, At5g43590; *pPLAIIIα*, At2g39220; *pPLAIIIβ*, At3g54950; *pPLAIIIγ*, At4g29800; *pPLAIIIδ*, At3g63200; *UBQ10*, At4g05320; and β-tubulin, At5g23860.

Supplemental Data

The following materials are available in the online version of this article.

Supplemental Figure 1. *pPLAIIIβ* Gene Expression at Various Stages of Development and in Response to Hormones and Abiotic Treatment.

Supplemental Figure 2. Seed Fatty Acid Composition and Stem Cuticular Wax Content in Wild-Type and *pPLAIIIβ*-Altered Plants.

Supplemental Figure 3. Morphological Changes by Altered *pPLAIIIβ*.

Supplemental Figure 4. Scanning Electron Micrographs of Epidermal Cell Morphology.

Supplemental Figure 5. Inhibition of Root Elongation by Treatment with Various Concentrations of Free Fatty Acid, 18:3.

Supplemental Figure 6. Ratio of Lipids with 36C in Acyl-Chains over Lipids with 34C in Acyl-Chains in Wild-Type, KO, OE, and COM Plants.

ACKNOWLEDGMENTS

We thank Mary Roth for technical work on the lipid analysis. This work was supported by grants from the National Science Foundation (MCB-0922879; IOS-0818740) and the USDA (2007-35318-18393). The Kansas Lipidomics Research Center's research was supported by grants from the National Science Foundation (MCB-0920663, DBI-0521587, and Kansas Experimental Program to Stimulate Competitive Research Award EPS-0236913), with support from the State of Kansas through the Kansas Technology Enterprise Corporation and Kansas State University, as well as from U.S. Public Health Service Grant P20 RR-016475 from the IDeA Network of Biomedical Research Excellence Program of the National Center for Research Resources.

Received November 11, 2010; revised February 9, 2011; accepted March 11, 2011; published March 29, 2011.

REFERENCES

Bosma, R., Miazek, K., Willemsen, S.M., Vermuë, M.H., and Wijffels, R.H. (2008). Growth inhibition of *Monodus subterraneus* by free fatty acids. Biotechnol. Bioeng. **101:** 1108–1114.

Burk, D.H., Liu, B., Zhong, R., Morrison, W.H., and Ye, Z.H. (2001). A katanin-like protein regulates normal cell wall biosynthesis and cell elongation. Plant Cell **13:** 807–827.

Devaiah, S.P., Roth, M.R., Baughman, E., Li, M., Tamura, P., Jeannotte, R., Welti, R., and Wang, X. (2006). Quantitative profiling of polar glycerolipid species from organs of wild-type Arabidopsis and a phospholipase Dα1 knockout mutant. Phytochemsitry **67:** 1907–1924.

Fan, L., Zheng, S., Cui, D., and Wang, X. (1999). Subcellular distribution and tissue expression of phospholipase phospholipase Dα, Dβ, and Dγ in Arabidopsis. Plant Physiol. **119:** 1371–1378.

Gao, W., Li, H.Y., Xiao, S., and Chye, M.L. (2010). Acyl-CoA-binding protein 2 binds lysophospholipase 2 and lysoPC to promote tolerance to cadmium-induced oxidative stress in transgenic Arabidopsis. Plant J. **62:** 989–1003.

Gu, Y., Kaplinsky, N., Bringmann, M., Cobb, A., Carroll, A., Sampathkumar, A., Baskin, T.I., Persson, S., and Somerville, C.R. (2010). Identification of a cellulose synthase-associated protein required for cellulose biosynthesis. Proc. Natl. Acad. Sci. USA **107:** 12866–12871.

He, Y., and Gan, S. (2002). A gene encoding an acyl hydrolase is involved in leaf senescence in *Arabidopsis*. Plant Cell **14:** 805–815.

Hong, Y., Devaiah, S.P., Bahn, S.C., Thamasandra, B.N., Li, M., Welti, R., and Wang, X. (2009). Phospholipase Dε and phosphatidic acid enhance Arabidopsis nitrogen signaling and growth. Plant J. **58:** 376–387.

Huang, S., Cerny, R.E., Bhat, D.S., and Brown, S.M. (2001). Cloning of an Arabidopsis patatin-like gene, STURDY, by activation T-DNA tagging. Plant Physiol. **125:** 573–584.

Jenkins, C.M., Yan, W., Mancuso, D.J., and Gross, R.W. (2006). Highly selective hydrolysis of fatty acyl-CoAs by calcium-independent phospholipase A_2β. Enzyme autoacylation and acyl-CoA-mediated reversal of calmodulin inhibition of phospholipase A2 activity. J. Biol. Chem. **281:** 15615–15624.

La Camera, S., Geoffroy, P., Samaha, H., Ndiaye, A., Rahim, G., Legrand, M., and Heitz, T. (2005). A pathogen-inducible patatin-like lipid acyl hydrolase facilitates fungal and bacterial host colonization in Arabidopsis. Plant J. **44:** 810–825.

Lamers, J.M.J., and Hülsmann, W.C. (1977). Inhibition of (Na^+ + K^+)-stimulated ATPase of heart by fatty acids. J. Mol. Cell. Cardiol. **9:** 343–346.

Li, M., Hong, Y., and Wang, X. (2009). Phospholipase D- and phosphatidic acid-mediated signaling in plants. Biochim. Biophys. Acta **1791:** 927–935.

Li, M., Qin, C., Welti, R., and Wang, X. (2006). Double knockouts of phospholipases Dζ1 and Dζ2 in Arabidopsis affect root elongation during phosphate-limited growth but do not affect root hair patterning. Plant Physiol. **140:** 761–770.

Li-Beisson, Y. (2010). Seed oil quantification. Acyl-Lipid Metabolism. In The Arabidopsis Book **8:** e0133, doi/10.1199/tab.0133.

Matos, A.R., and Pham-Thi, A.T. (2009). Lipid deacylating enzymes in plants: old activities, new genes. Plant Physiol. Biochem. **47:** 491–503.

Mauseth, J.D. (1988). Plant Anatomy. (Menlo Park, CA: Benjamin/Cummings Publishing).

Meijer, H.J., and Munnik, T. (2003). Phospholipid-based signaling in plants. Annu. Rev. Plant Biol. **54:** 265–306.

Ohkawa, M., and Nishikawa, Y. (1987). Plant growth inhibitory activity of fatty acids and the related compounds by the *Avena Coleoptiles* test. Plant Sci. **53:** 35–38.

Ollis, D.L., et al. (1992). The α/β hydrolase fold. Protein Eng. **5:** 197–211.

Pan, X., and Wang, X. (2009). Profiling of plant hormones by mass spectrometry. J. Chromatogr. B Analyt. Technol. Biomed. Life Sci. **877:** 2806–2813.

Pan, X., Welti, R., and Wang, X. (2008). Simultaneous quantification of major phytohormones and related compounds in crude plant extracts by liquid chromatography-electrospray tandem mass spectrometry. Phytochemistry **69:** 1773–1781.

Pan, X., Welti, R., and Wang, X. (2010). Quantitative analysis of major plant hormones in crude plant extracts by high-performance liquid chromatography-mass spectrometry. Nat. Protoc. **5:** 986–992.

Pappan, K., Zheng, L., Krishnamoorthi, R., and Wang, X. (2004). Evidence for and characterization of Ca^{2+} binding to the catalytic region of *Arabidopsis thaliana* phospholipase Dβ. J. Biol. Chem. **279:** 47833–47839.

Raymer, G., Willard, J.M., and Schottel, J.L. (1990). Cloning, sequencing, and regulation of expression of an extracellular esterase gene from the plant pathogen *Streptomyces scabies*. J. Bacteriol. **172:** 7020–7026.

Rietz, S., Dermendjiev, G., Oppermann, E., Tafesse, F.G., Effendi, Y., Holk, A., Parker, J.E., Teige, M., and Scherer, G.F. (2010). Roles of Arabidopsis patatin-related phospholipases A in root development are related to auxin responses and phosphate deficiency. Mol. Plant **3:** 524–538.

Rietz, S., Holk, A., and Scherer, G.F. (2004). Expression of the patatin-related phospholipase A gene AtPLA IIA in *Arabidopsis thaliana* is up-regulated by salicylic acid, wounding, ethylene, and iron and phosphate deficiency. Planta **219:** 743–753.

Rowland, O. (2010). Analysis of cuticular waxes. Acyl-Lipid Metabolism. In The Arabidopsis Book **8:** e0133, doi/10.1199/tab.0133.

Ryu, S.B. (2004). Phospholipid-derived signaling mediated by phospholipase A in plants. Trends Plant Sci. **9:** 229–235.

Scherer, G.F., Ryu, S.B., Wang, X., Matos, A.R., and Heitz, T. (2010). Patatin-related phospholipase A: Nomenclature, subfamilies and functions in plants. Trends Plant Sci. **15:** 693–700.

Six, D.A., and Dennis, E.A. (2000). The expanding superfamily of phospholipase $A_{(2)}$ enzymes: Classification and characterization. Biochim. Biophys. Acta **1488:** 1–19.

Swann, A.C. (1984). Free fatty acids and (Na^+,K^+)-ATPase: Effects on cation regulation, enzyme conformation, and interactions with ethanol. Arch. Biochem. Biophys. **233:** 354–361.

Swarts, H.G., Van Uem, T.J., Hoving, S., Fransen, J.A., and De Pont, J.J. (1991). Effect of free fatty acids and detergents on H,K-ATPase. The steady-state ATP phosphorylation level and the orientation of the enzyme in membrane preparations. Biochim. Biophys. Acta **1070:** 283–292.

Tilton, G.B., Shockey, J.M., and Browse, J. (2004). Biochemical and molecular characterization of ACH2, an acyl-CoA thioesterase from *Arabidopsis thaliana*. J. Biol. Chem. **279:** 7487–7494.

Tso, T.C. (1964). Plant-growth inhibition by some fatty acids and their analogues. Nature **202:** 511–512.

Tsuzuki, E., Yamamoto, Y., and Shimizu, T. (1987). Fatty acids in Buckwheat are growth inhibitors. Ann. Bot. (Lond.) **60:** 69–70.

Updegraff, D.M. (1969). Semimicro determination of cellulose in biological materials. Anal. Biochem. **32:** 420–424.

Wang, X. (2001). Plant phospholipases. Annu. Rev. Plant Physiol. Plant Mol. Biol. **52:** 211–231.

Welti, R., Li, W., Li, M., Sang, Y., Biesiada, H., Zhou, H.E., Rajashekar, C.B., Williams, T.D., and Wang, X. (2002). Profiling membrane lipids in plant stress responses. Role of phospholipase Dα in freezing-induced lipid changes in Arabidopsis. J. Biol. Chem. **277:** 31994–32002.

Xiao, S., Gao, W., Chen, Q.F., Chan, S.W., Zheng, S.X., Ma, J., Wang, M., Welti, R., and Chye, M.L. (2010). Overexpression of *Arabidopsis* acyl-CoA binding protein ACBP3 promotes starvation-induced and age-dependent leaf senescence. Plant Cell **22:** 1463–1482.

Yang, W., Devaiah, S.P., Pan, X., Isaac, G., Welti, R., and Wang, X. (2007). AtPLAI is an acyl hydrolase involved in basal jasmonic acid production and Arabidopsis resistance to *Botrytis cinerea*. J. Biol. Chem. **282:** 18116–18128.

Zhong, R., Kays, S.J., Schroeder, B.P., and Ye, Z.H. (2002). Mutation of a chitinase-like gene causes ectopic deposition of lignin, aberrant cell shapes, and overproduction of ethylene. Plant Cell **14:** 165–179.

Patatin-Related Phospholipase pPLAIIIβ-Induced Changes in Lipid Metabolism Alter Cellulose Content and Cell Elongation in *Arabidopsis*

Maoyin Li, Sung Chul Bahn, Liang Guo, William Musgrave, Howard Berg, Ruth Welti and Xuemin Wang

Plant Cell 2011;23;1107-1123; originally published online March 29, 2011;
DOI 10.1105/tpc.110.081240